A Note about Self-Induced Velocity Generated by a Lifting-Line Wing or Rotor Blade

Franklin D. Harris
University of Maryland
Dept. of Aerospace Engineering, College Park, Maryland

February 2006

Since its founding, NASA has been dedicated to the advancement of aeronautics and space science. The NASA Scientific and Technical Information (STI) Program Office plays a key part in helping NASA maintain this important role.

The NASA STI Program Office is operated by Langley Research Center, the Lead Center for NASA's scientific and technical information. The NASA STI Program Office provides access to the NASA STI Database, the largest collection of aeronautical and space science STI in the world. The Program Office is also NASA's institutional mechanism for disseminating the results of its research and development activities. These results are published by NASA in the NASA STI Report Series, which includes the following report types:
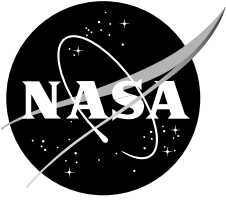
- TECHNICAL PUBLICATION. Reports of completed research or a major significant phase of research that present the results of NASA programs and include extensive data or theoretical analysis. Includes compilations of significant scientific and technical data and information deemed to be of continuing reference value. NASA's counterpart of peer-reviewed formal professional papers but has less stringent limitations on manuscript length and extent of graphic presentations.

- TECHNICAL MEMORANDUM. Scientific and technical findings that are preliminary or of specialized interest, e.g., quick release reports, working papers, and bibliographies that contain minimal annotation. Does not contain extensive analysis.

- CONTRACTOR REPORT. Scientific and technical findings by NASA-sponsored contractors and grantees.

- CONFERENCE PUBLICATION. Collected papers from scientific and technical conferences, symposia, seminars, or other meetings sponsored or cosponsored by NASA.

- SPECIAL PUBLICATION. Scientific, technical, or historical information from NASA programs, projects, and missions, often concerned with subjects having substantial public interest.

- TECHNICAL TRANSLATION. English-language translations of foreign scientific and technical material pertinent to NASA's mission.

Specialized services that complement the STI Program Office's diverse offerings include creating custom thesauri, building customized databases, organizing and publishing research results . . . even providing videos.

For more information about the NASA STI Program Office, see the following:

- Access the NASA STI Program Home Page at *http://www.sti.nasa.gov*

- E-mail your question via the Internet to help@sti.nasa.gov

- Fax your question to the NASA Access Help Desk at (301) 621-0134

- Telephone the NASA Access Help Desk at (301) 621-0390

- Write to:
  NASA Access Help Desk
  NASA Center for AeroSpace Information
  7121 Standard Drive
  Hanover, MD 21076-1320

A Note about Self-Induced Velocity Generated by a Lifting-Line Wing or Rotor Blade

Franklin D. Harris
University of Maryland
Dept. of Aerospace Engineering, College Park, Maryland

February 2006

Available from:

Table of Contents

Preface

This note serves as an elementary introduction to the induced velocity created by a field of vortices that reside in the wake of a rotor blade. The approach is to build a bridge between familiar fixed-wing theory over to a rotor blade in forward flight. This bridge is built in four parts plus concluding remarks.

By way of background, rotorcraft technologists, after a nearly seven decade effort, have finally begun to provide accurate computer based prediction of a helicopter rotor blade's airloads and dynamic response. The decades-long effort was capped during the last four years by tying airload prediction (with advanced CFD methods) to completely coupled structural dynamic response (calculated with very advanced modal methods). Typical results, such as Refs. 1 and 2, confirm the progress of what this relatively small band of engineers have achieved after some 70 years of dedicated work.

In September 1969, I presented a paper at the V/STOL Technology and Planning Conference sponsored by the Air Force Flight Dynamics Laboratory (Ref. 3).[1] This paper included a figure showing the progress in removing assumptions from the original rotor performance theory developed by Juan de la Cierva in the late 1920s. The figure is reproduced in this note as Figure 1. You can see from Fig. 1's dashed line that I was, in 1969, confident that by 1975 we would be done. Of course, a revision to that 1969 view reflecting history is quite in order. So, Fig.1's solid line now shows the more accurate progress in hindsight.

One of the toughest assumptions to remove was that of uniform downwash. Professor Rene Miller of MIT showed the way in 1962 with Ref. 4. Work that followed is discussed rather completely in Chapter 13 of Wayne Johnson's *Helicopter Theory*. The interaction between the rotor blades that create the induced velocity field and the effect the induced velocity feeds back on each blade was a daunting complexity that needed a computer before even rudimental solutions became tractable.

There is some interesting knowledge to be gained, however, from disconnecting the blade loading from the induced field. That is the purpose of this note: to calculate the induced velocity at a blade where the blade's bound circulation is given in terms of radius and azimuth. Once specified, the blade's bound circulation and lift distribution remain unchanged despite the resulting induced velocity field. This is, of course, a comparatively simple problem compared to the real problem. Furthermore, in this note only a one-bladed rotor is considered, and to make the problem even simpler, only a prescribed, rigid wake is considered.

An interesting advantage of these simplifications is that a bridge from the fixed wing to the rotary wing is quite easy to construct. To make the bridge secure, I have tried to leave nothing to the imagination concerning the sign conventions, the mathematical notations, and the steps under discussion.

<div align="right">F. D. Harris, Oct. 16, 2005</div>

---

[1] This conference was held in Las Vegas, Nevada, a city—I was led to believe—that was the V/STOL technical capital of the world.

I. Introduction to the Fixed Wing

The Classical Fixed-Wing Problem

The classical fixed-wing induced velocity problem begins, as explained in most aerodynamic textbooks, by assuming a bound circulation that is elliptical. The wing is placed in straight and level flight. An array of horseshoe vortices is envisioned. The resulting induced velocity at the wing is found to be constant from the port wingtip to the starboard wingtip. In summary,

$$(0.1) \quad \text{if} \quad \Gamma_{xw} = \Gamma_o \sqrt{1 - \left(\frac{2xw}{b} \right)^2} \quad \text{then} \quad v_{xw} = \frac{\Gamma_o}{2b}$$

where Γ_o is the maximum circulation in square feet per second, b is the wingspan in feet, and xw is the span station being $xw = -b/2$ at the port wingtip and $xw = +b/2$ at the starboard wingtip. The induced velocity, v_{xw}, is in feet per second and is constant from tip to tip.

In this note, think of the wing rotating, not flying straight. Therefore it is quite helpful to approach the fundamental geometry used in the classical derivation from a different point of view. Suppose a fixed wing is east of a pylon and flying north past the pylon. Ignore—for the moment—an anticipated 180-degree U-turn around the pylon.[2] (The U-turn results will be discussed after reconstructing the classical problem.) The situation is illustrated with Fig. 2.

In Fig. 2, the right-hand axis system gives a positive Z axis coming up out of the paper. The "pylon" is located at $X = Y = Z = 0$. The wing centerline is placed a distance D from the pylon in the plus X direction. The wing coordinates are measured from the wing centerline. The station on the wing where induced velocity is sought is denoted by xw. A vortex trails downstream from the wing at wing station xv. A small element of the vortex, dS, is shown located at a distance L from wing station xw. The reference angle θ is used to locate the vortex element in relation to the wing. When θ is equal to minus $\pi/2$, the vortex element is at $-\infty$. When θ equals zero, the vortex element is located at the wing. The calculation of induced velocity by the Biot-Savart law, as derived from vector notation, is simply

$$(0.2) \quad d\left(dv_{xw} \right) = \frac{\gamma_v}{4\pi} \left[\frac{L_i dS_j - L_j dS_i}{L^3} \right] d\theta = \frac{1}{4\pi} \left[-\left(\frac{d\Gamma_{xw}}{dxw} \right) dxv \right]_{xw=xv} \left[\frac{L_i dS_j - L_j dS_i}{L^3} \right] d\theta$$

This fundamental equation is deceptively simple because to calculate the induced velocity, v_{xw}, at any station along the wing, xw, only a double integral has to be performed. That is

$$(0.3) \quad v_{xw} = \frac{1}{4\pi} \int_{-b/2}^{+b/2} \int_{-\pi/2}^{0} \left[-\left(\frac{d\Gamma_{xw}}{dxw} \right) dxv \right]_{xw=xv} \left[\frac{L_i dS_j - L_j dS_i}{L^3} \right] d\theta$$

---

[2] Imagine a rotor blade at the traditional downwind, zero-azimuth station, which will, after the U-turn, be at the 180-degree upwind azimuth station.

The double integration required by Eq. (0.3) is hampered (to put it mildly) whenever $\frac{d\Gamma_{xw}}{dxw}$ equals either plus or minus infinity. The double integration can be an even bigger problem whenever $L = 0$. If the double integration is performed numerically, situations where numbers approach plus or minus 10^{10} can become quite frustrating. Modern computers using so-called double precision and advanced numerical integration schemes have helped to lower this frustration. But the fundamental basis of numerical integration is the Taylor series. The hope is that—without a breach in engineering accuracy—$d\theta$ and dxw can be replaced by $\Delta\theta$ and Δxw when the integral operators are replaced by summation operators. There are, of course, a number of ingenious coordinate transformations that can completely remove an apparent integrating roadblock.

Here is an example of a coordinate transformation that helps lower frustrations with the fixed-wing problem. Consider the situation when a wing's lifting line is loaded with an elliptical bound circulation defined as

$$(0.4) \quad \Gamma_{xw} = \Gamma_o \sqrt{1 - \left(\frac{2xw}{b}\right)^2}$$

where $xw = -b/2$ at the port wingtip and $xw = +b/2$ at the starboard wingtip. The derivative that the Biot-Savart law requires is

$$(0.5) \quad \gamma_v = -\left(\frac{d\Gamma_{xw}}{dxw} dxw\right)_{xw=xv} = -\left\{\frac{1}{2}\Gamma_o\left[1-\left(\frac{2xv}{b}\right)^2\right]^{-\frac{1}{2}}\left[-2\left(\frac{2xv}{b}\right)\right]\left(\frac{2}{b}dxv\right)\right\} = +\frac{2}{b}\left[\frac{\Gamma_o}{\sqrt{1-\left(\frac{2xv}{b}\right)^2}}\right]\left(\frac{2xv}{b}\right)dxv$$

where $xv = -b/2$ at the port wingtip and $xv = +b/2$ at the starboard wingtip. You can immediately see that the required derivative is plus infinity at the starboard wingtip and minus infinity at the port wingtip. Now look what happens with the coordinate transformation of

$$(0.6) \quad xv = -\frac{b}{2}\cos\beta \qquad \text{and} \qquad dxv = \frac{b}{2}\sin\beta \, d\beta$$

where $\beta = 0$ is the port wingtip and $\beta = \pi$ is the starboard wingtip. Then the bound circulation becomes

$$(0.7) \quad \Gamma_\beta = \Gamma_o \sqrt{1-\left(\frac{2}{b}\right)^2\left(-\frac{b}{2}\cos\beta\right)^2} = \Gamma_o\sqrt{1-\cos^2\beta} = \Gamma_o\sin\beta$$

and the required Biot-Savart derivative becomes

$$(0.8) \quad \gamma_v = -\left(\frac{d\Gamma_{xw}}{dxw}dxv\right)_{xw=xv} = \frac{2}{b}\left[\frac{\Gamma_o}{\sqrt{1-\cos^2\beta}}\right](-\cos\beta)\left(\frac{b}{2}\sin\beta \, d\beta\right) = -\Gamma_o\cos\beta \, d\beta$$

2

Clearly, singularities caused by the derivative $\dfrac{d\Gamma_{xw}}{dxw}$ at the wingtips have been removed.

The preceding coordinate transformation, when placed in the Biot-Savart law for this fixed-wing problem, gives

$$(0.9) \quad v_{xw} = \frac{1}{4\pi} \int_0^\pi \int_{-\pi/2}^0 [-\Gamma_o \cos\beta \, d\beta] \left[\frac{L_i dS_j - L_j dS_i}{L^3} \right] d\theta$$

The next step is to construct the second portion of the integrand, which is

$$\left[\frac{L_i dS_j - L_j dS_i}{L^3} \right] d\theta$$

The geometric dimensions, L, L_i, L_j, dS_i and dS_j , are components of vectors. When looking at Fig. 2, one has a choice of reference systems. Since this fixed wing is flying straight and level past the pylon, there is no advantage to including the distance D or using the reference angle θ in the wake geometry.[3] Therefore, continue using just the reference angle δ. That means

$$\left[\frac{L_i dS_j - L_j dS_i}{L^3} \right] d\theta \quad \text{is replaced by} \quad \left[\frac{L_i dS_j - L_j dS_i}{L^3} \right] d\delta$$

and δ is positive counterclockwise. The vortex segment farthest downstream is located at $\delta = 0$ and a vortex segment right at the wing is located by $\delta = +\pi/2$.

Now, from Fig. 2, the distance L is written as

$$L = L_i + L_j + L_k = (Xw - Xv)i + (Yw - Yv)j + (Zw - Zv)k$$

$$(0.10)$$

$$\text{with} \quad Xw = xw \qquad\qquad Yw = 0 \qquad\qquad\qquad Zw = 0$$

$$Xv = xv \qquad\qquad Yv = \frac{xv - xw}{\tan\delta} \qquad\qquad Zv = 0$$

$$\text{and} \quad L^3 = \left[(Xw - Xv)^2 + (Yw - Yv)^3 + (Zw - Zv)^2 \right]^{3/2}$$

Therefore, with the usual "substitute and simplify" phrase,

$$(0.11) \quad L^3 = \left[\frac{(xv - xw)^2}{\sin^2 \delta} \right]^{3/2}$$

In a similar manner, the vortex is described by the vector

$$(0.12) \quad S = S_i + S_j + S_k = (Xv)i + (Yv)j + (Zv)k$$

---

[3] The next part of this note addresses the U-turning wing. That problem requires, of course, some reference system that includes D and uses the reference angle θ.

and therefore

$$dS_i = \frac{\partial S_i}{\partial \delta} d\delta = \frac{\partial Xv}{\partial \delta} d\delta = 0$$

$$(0.13) \quad dS_j = \frac{\partial S_j}{\partial \delta} d\delta = \frac{\partial Yv}{\partial \delta} d\delta = \frac{(xv - xw)}{\sin^2 \delta}$$

$$dS_k = \frac{\partial S_k}{\partial \delta} d\delta = \frac{\partial Zv}{\partial \delta} d\delta = 0$$

Here the assumption about the trailed vortex geometry is that it extends straight aft of the wing without descending or climbing, remaining perpendicular to the wing lifting line. Again, by substitution and simplification,

$$(0.14) \quad \left[\frac{L_i dS_j - L_j dS_i}{L^3} \right] d\delta = \frac{-1}{xv - xw} \sin \delta \, d\delta$$

The double integral created by the Biot-Savart law now appears, after substituting Eq. (0.14) into Eq. (0.9), as

$$(0.15) \quad v_{xw} = \frac{1}{4\pi} \int_0^\pi \int_0^{\pi/2} \left[-\Gamma_o \cos \beta \, d\beta \right] \left[\frac{-1}{xv - xw} \sin \delta \right] d\delta$$

A minor problem is immediately observed in Eq. (0.15). Formal integration really requires that xv and xw be related, in some fashion, to β and/or δ. This minor problem is repaired using Eq. (0.6) where $xv = -\frac{b}{2} \cos \beta$. And, rather than have the vortex wing station keyed by the angle β while the wing station is keyed to xv, you can make the substitution that $xw = -\frac{b}{2} \cos \alpha$. These substitutions result in

$$(0.16) \quad v_\alpha = \frac{1}{2b\pi} \int_0^\pi \int_0^{\pi/2} \left[-\Gamma_o \cos \beta \, d\beta \right] \left[\frac{-1}{\cos \alpha - \cos \beta} \sin \delta \right] d\delta$$

A much, much bigger problem with Eq. (0.15) and Eq. (0.16) is that any integration, whether formal or numerical, must face the possibility that (xv – xw) might be zero. In Eq. (0.16) terms, real trouble will occur if $\beta = \alpha$.

The integration with respect to wake age (i.e., with respect to δ) results in

$$(0.17) \quad v_\alpha = \frac{\Gamma_o}{2b\pi} \int_0^\pi \left[\frac{\cos \beta}{\cos \alpha - \cos \beta} \right] d\beta = -\frac{\Gamma_o}{2b\pi} \int_0^\pi \left[\frac{\cos \beta}{\cos \beta - \cos \alpha} \right] d\beta = -\frac{\Gamma_o}{2b}$$

Note immediately that the above derivation gives a negative value for induced velocity created by a wing carrying positive lift! The reason for this outcome is the right-hand rule axis system of Fig. 2

4

where the Z axis is positive up. Therefore, the induced velocity is directed in the negative Z direction. Of course, reason prevails in all textbooks on the subject, so the negative induced velocity is simply called downwash and the sign is changed to positive. This is equivalent to letting $\gamma_v = +\Gamma_o \cos\beta \, d\beta$.

Incidentally, Glauert proved the integration with respect to β equals π long ago. Also, Alan Pope in Appendix 3 of his book *Basic Wing and Airfoil Theory* shows that

(0.18)
$$
\begin{aligned}
v_\alpha &= \frac{\Gamma_o}{2b\pi} \int_0^\pi \left[\frac{\cos\beta}{\cos\beta - \cos\alpha} \right] d\beta = \frac{\Gamma_o}{2b\pi} \int_0^\pi \left[1 + \frac{\cos\alpha}{\cos\beta - \cos\alpha} \right] d\beta \\
&= \frac{\Gamma_o}{2b\pi} \int_0^\pi d\beta + \frac{\Gamma_o}{2b\pi} \cos\alpha \int_0^\pi \left[\frac{1}{\cos\beta - \cos\alpha} \right] d\beta = \frac{\Gamma_o}{2b\pi}[\pi] + \frac{\Gamma_o}{2b\pi} \cos\alpha [0]
\end{aligned}
$$

It comes in very handy at times to know that

(0.19) $\quad \displaystyle\int_0^\pi \left[\frac{1}{\cos\beta - \cos\alpha} \right] d\beta \equiv 0 \qquad$ and that $\quad \displaystyle\int_0^\pi \left[\frac{\cos n\beta}{\cos\beta - \cos\alpha} \right] d\beta \equiv \frac{\pi \sin n\beta}{\sin\beta}$

But now suppose numerical integration (rather than formal, closed-form integration) of Eq. (0.16) is the solution approach. I took an approach with the Mathsoft Inc. product called Mathcad Plus 6.0 that goes like this:

$$\Gamma_o = 2 \qquad\qquad b = 1$$

$$s = 0, 1 \ldots\ldots 179$$

$$\alpha_s = (s + 1/2)\frac{\pi}{180}$$

$$dvd\beta d\delta_{n,m} = \frac{\Gamma_o}{2b\pi} \left\{ \frac{\cos\beta_m}{\cos\beta_m - \cos\alpha_s} \right\} \sin\delta_n$$

$$n = 0, 1 \ldots\ldots 90 \qquad\qquad \delta_n = \frac{\pi}{180} n$$

$$m = 0, 1 \ldots\ldots 180 \qquad\qquad \beta_m = \frac{\pi}{180} m$$

$$dvd\beta_m = \frac{\pi}{180} \sum_{n=0}^{89} \frac{dvd\beta d\delta_{n,m} + dvd\beta d\delta_{n+1,m}}{2}$$

$$v_s = \frac{\pi}{180} \sum_{n=0}^{179} \frac{dvd\beta_m + dvd\beta_{m+1}}{2}$$

$$xw_s = -\frac{b}{2} \cos\alpha_s$$

This numerical solution, "programmed" in Mathcad, gave +0.9999746151 accuracy nearly within a blink of an eye, using a Dell Optiplex high-end computer. The answer from Eq. (0.17) is exactly unity (when you ignore the minus sign).

As a reminder, the fixed wing represented by a lifting line and an elliptical bound circulation produces a lift calculated from

$$
\begin{aligned}
L &= \rho V \Gamma_o \int_{-b/2}^{+b/2} \sqrt{1 - \left(\frac{2xw}{b}\right)^2} \, dxw \\
&= \rho V \Gamma_o \int_{-\pi/2}^{+\pi/2} \sqrt{1 - \sin^2 \theta} \left(\frac{b}{2} \cos \theta \, d\theta\right) \\
&= \rho V \Gamma_o \frac{b}{2} \int_{-\pi/2}^{+\pi/2} \cos^2 \theta \, d\theta \\
&= \rho V \Gamma_o \frac{b}{2} \left(\frac{\pi}{2}\right) \\
&= \frac{\pi}{4} \rho b V \Gamma_o \qquad \text{so} \qquad \Gamma_o = \frac{4L}{\pi \rho b V}
\end{aligned}
$$

(0.20)

The wing incurs an induced drag to carry this lift, which is

$$
(0.21) \quad \text{Induced drag} = L \frac{V_{xw}}{V} = \left(\frac{\pi}{4} \rho b V \Gamma_o\right)\left(\frac{\Gamma_o}{2bV}\right) = \frac{\pi}{8} \rho \Gamma_o^2 = \frac{L^2}{(\rho/2) V^2 \pi b^2}
$$

This drag can be used to calculate a horsepower required by multiplying both sides of the equation by velocity, V, and dividing by 550. Thus,

$$
(0.22) \quad \text{Induced Horsepower} \equiv HP_i = \frac{V}{550}\left[\frac{L^2}{(\rho/2) V^2 \pi b^2}\right] = \frac{Vq}{550\pi}\left(\frac{L}{qb^2}\right)^2 \quad \text{with } q = (\rho/2) V^2
$$

A numerical example calculated here will be a useful result to which one can later compare rotating-wing calculations. Suppose both a wing and a rotor have equal span, say, 44 feet. In rotor notation, the rotor radius is 22 feet. Assume, for example, that each lifting device carries a lift of 2,712 pounds, each is flying at sea level ($\rho = 0.002378$ slug/ft^2), and each is flying at V = 301.8 ft/sec or 178 knots. Then, by Eq. (0.22), the induced horsepower required by the wing is 6.13 horsepower.

Keep in mind that the elliptical bound circulation distribution used in the above discussion is the first term of the more general distribution used in fixed-wing analyses. Recall that the general distribution is seen in the form

$$
(0.23) \quad \Gamma = 2bV \sum_{1}^{\infty} A_n \sin n\beta
$$

Everything read in this note—including the rotor analyses—could be extended by this fixed-wing logic of Eq. (0.23).

And there you have the fixed wing flying north past the pylon located off its port wingtip. Now consider the situation after the fixed wing does a 180-degree U-turn.

The Fixed Wing after Completing a 180-Degree U-Turn

The next step in bridging the gap between a fixed wing and a rotary wing was actually taken by H. Glauert in 1923, although it is doubtful he had a bridge in mind when he published R & M 866. After all, in 1923, Juan de la Cierva's earliest autogyro experiments were just bearing fruit in Spain and a practical helicopter was still 15 years away. The title of Glauert's 1923 report is "Calculation of the Rotary Derivatives Due to Yawing for a Monoplane Wing." He was dealing with the wing rolling and yawing moments created by an induced velocity field that trailed the wing in one half of a circle. The problem is, in fact, quite akin to a hovering one-bladed rotor where only a small part of the wake is taken into account. Glauert obtained a very simple closed-form solution by assuming the wing made the U-turn with a large turning radius, D, relative to the wingspan, b, (i.e., D>>b). His quite useable engineering result for the induced velocity over the wingspan was (in the notations of my note here)

$$(0.24) \qquad v_{xw} = \frac{\Gamma_o}{2b}\left(1 + \frac{1}{2}\frac{xw}{D}\right)$$

The purpose of this portion of the note is to explore this problem when the turning radius is considerably smaller than what Glauert assumed. The objective is to think of the "pylon" as a rotor hub and place the port wingtip a small distance from the hub, which gives the appearance of a "root cutout" in rotorcraft terminology. Glauert's approach will be presented first and then a numerical integrating approach will be shown.

The geometry of the problem is illustrated with Fig. 3. In contrast to Fig. 2, the wing has now advanced 180 degrees. *Immediately note* that the X axis is positive to the left, but left the Y axis in its commonly found, ordinate position. By the righthand rule then, the positive Z axis now points down, which is into the paper. The wing is doing a U-turn of distance D, which is measured from the "pylon" to the wing mid-span point. The wing is represented by a lifting-line vortex having an elliptical bound circulation, just as with the classical fixed-wing problem. The Biot-Savart law is again invoked, so

$$(0.25) \qquad d\left(dv_{xw}\right) = \frac{\gamma_v}{4\pi}\left[\frac{L_i dS_j - L_j dS_i}{L^3}\right]d\theta$$

and the dimensions are expressed as vectors. However, the basic vortex geometry has changed in going from Fig. 2 to Fig. 3. Now

$$L = L_i + L_j + L_k = (Xw - Xv)i + (Yw - Yv)j + (Zw - Zv)k$$

$$(0.26)$$
$$\text{where} \quad Xw = D + xw \qquad\qquad Yw = 0 \qquad\qquad Zw = 0$$
$$Xv = (D + xv)\cos\theta \qquad Yv = -(D + xv)\sin\theta \qquad Zv = 0$$

$$\text{and} \quad L^3 = \left[(Xw - Xv)^2 + (Yw - Yv)^3 + (Zw - Zv)^2\right]^{3/2}$$

The reference angle θ is taken positive counterclockwise in Fig. 3. In a similar manner, the vortex is described by

(0.27) $S = S_i + S_j + S_k = (Xv)i + (Yv)j + (Zv)k$

but with changed vortex geometry reflecting the ½-circle wake, the vortex element geometry is

$$dS_i = \frac{\partial S_i}{\partial \theta} d\theta = \frac{\partial Xv}{\partial \theta} d\theta = \frac{\partial (D+xv)\cos\theta}{\partial \theta} d\theta = -(D+xv)\sin\theta$$

(0.28) $$dS_j = \frac{\partial S_j}{\partial \theta} d\theta = \frac{\partial Yv}{\partial \theta} d\theta = \frac{\partial[-(D+xv)]\sin\theta}{\partial \theta} d\theta = -(D+xv)\cos\theta$$

$$dS_k = \frac{\partial S_k}{\partial \theta} d\theta = \frac{\partial Zv}{\partial \theta} d\theta = 0$$

Here the assumption about the trailed vortex geometry is that it extends in a circular arc aft of the wing for 180 degrees without descending or climbing. Furthermore, any given vortex has constant circulation, γ_v , from when it leaves the wing all the way back to when the turn began (i.e., $\theta = 0$ back to $\theta = -\pi$).

The substitution of this U-turn geometry into the Biot-Savart law gives, with simplification,

(0.29) $$d(dv_{xw}) = \frac{\gamma_v}{4\pi} \left\{ \frac{(D+xv)(D+xw)\cos\theta - (D+xv)^2}{\left[(D+xv)^2 + (D+xw)^2 - 2(D+xv)(D+xw)\cos\theta\right]^{3/2}} \right\} d\theta$$

The wake-age integral problem is immediately seen as requiring elliptical integrals—even if the wing's bound vortex circulation varies with wake age. For this example, assume as Glauert did, that γ_v does not vary with θ. Now, at the risk of boring you, the transformation to complete elliptical integrals (i.e., E and K) begins by letting $\theta = \pi - 2\phi$ and $d\theta = -2\,d\phi$. You also need to recall that

$$\cos\theta = \cos(\pi - 2\phi) = -\cos(2\phi) = 2\sin^2\phi - 1$$

Then, a couple of substitutions and rearrangements immediately shows that

(0.30)

$$d(dv_{xw}) = \frac{\gamma_v}{4\pi} \frac{2(D+xv)(2D+xw+xv)}{(2D+xw+xv)^{3/2}} \left\{ \frac{1}{\left[1-k^2\sin^2\phi\right]^{3/2}} \right\} d\phi -$$

$$- \frac{\gamma_v}{4\pi} \frac{4(D+xv)(D+xw)}{(2D+xw+xv)^{3/2}} \left\{ \frac{\sin^2\phi}{\left[1-k^2\sin^2\phi\right]^{3/2}} \right\} d\phi$$

where

(0.31) $$k^2 = \frac{4(D+xw)(D+xv)}{(2D+xv+xw)^2}$$

This substitution changes the wake-age integrating limits from $\theta = -\pi$ to $\theta = 0$ over to $\phi = 0$ to $\phi = +\pi/2$. The two budding integrals can be found, for example, in the translated Russian

handbook by I. S. Gradshteyn and I. M. Ryzhik titled *Tables of Integrals, Series, and Products*, edited by Alan Jeffrey. Thus

$$\int_0^{\pi/2} \frac{1}{\left[1-k^2\sin^2\phi\right]^{3/2}}\,d\phi = \frac{1}{1-k^2}E$$

$$(0.32) \quad \int_0^{\pi/2} \frac{\sin^2\phi}{\left[1-k^2\sin^2\phi\right]^{3/2}}\,d\phi = \int_0^{\pi/2} \frac{1}{\left[1-k^2\sin^2\phi\right]^{3/2}}\,d\phi - \int_0^{\pi/2} \frac{\cos^2\phi}{\left[1-k^2\sin^2\phi\right]^{3/2}}\,d\phi$$

$$= \frac{1}{1-k^2}E - \left(\frac{1}{k^2}K - \frac{1}{k^2}E\right)$$

where the complete elliptical integrals, E and K, are computed as

$$(0.33) \quad E = \int_0^{\pi/2}\sqrt{1-k^2\sin^2\phi}\,d\phi \qquad\qquad K = \int_0^{\pi/2}\frac{1}{\sqrt{1-k^2\sin^2\phi}}\,d\phi$$

and their values depend on the modulus, k^2, which for this U-turning wing problem, is given by Eq. (0.31). Note that when $xv = xw$, $k^2 = 1.0$, $E = 1.0$, and $K = +\infty$.

In this way

$$(0.34) \quad dv_{xw} = \frac{\gamma_v}{4\pi}\int_{-\pi}^0 \left\{\frac{(D+xv)(D+xw)\cos\theta - (D+xv)^2}{\left[(D+xv)^2+(D+xw)^2-2(D+xv)(D+xw)\cos\theta\right]^{3/2}}\right\}d\theta$$

is converted into

$$dv_{xw} = \frac{\gamma_v}{4\pi}\frac{2(D+xv)(2D+xw+xv)}{(2D+xw+xv)^{3/2}}\int_0^{\pi/2}\left\{\frac{1}{\left[1-k^2\sin^2\phi\right]^{3/2}}\right\}d\phi -$$

$$(0.35)$$

$$-\frac{\gamma_v}{4\pi}\frac{4(D+xv)(D+xw)}{(2D+xw+xv)^{3/2}}\int_0^{\pi/2}\left\{\frac{\sin^2\phi}{\left[1-k^2\sin^2\phi\right]^{3/2}}\right\}d\phi$$

which, upon simplification, reduces to

$$(0.36) \quad dv_{xw} = \frac{\gamma_v}{4\pi}\left[\frac{E}{xv-xw}+\frac{K}{2D+xv+xw}\right]$$

The wake integration being complete, the problem is reduced to the spanwise collection of all vortices trailed from the wing.

The insightful step Glauert next took was to make use of the approximations for E and K when k^2 is closer to 1.0 than to 0 rather than calculate them using Eq. (0.33). These approximations are

$$(0.37) \quad E \approx 1 + \frac{1}{4}\left(\ln\left(\frac{16}{1-k^2}\right) - \frac{1}{2} \right)\left(1-k^2\right)$$

$$K \approx \frac{1}{2}\ln\left(\frac{16}{1-k^2}\right) + \frac{1}{8}\left(\ln\left(\frac{16}{1-k^2}\right) - 1 \right)\left(1-k^2\right)$$

The fact that the approximation for E begins with one (1) is enormously important, which is seen when these approximations are substituted into Eq. (0.36). Of course, a lengthy integration problem results, which is

$$(0.38) \quad
\begin{aligned}
v_{xw} = &\int_{-b/2}^{+b/2} \frac{\gamma_v}{4\pi}\left(\frac{1}{xv - xw}\right) \\
&+ \int_{-b/2}^{+b/2} \frac{\gamma_v}{4\pi}\left(\frac{1}{xv - xw}\right)\left[\frac{1}{4}\left(\ln\left(\frac{16}{1-k^2}\right) - \frac{1}{2}\right)\left(1-k^2\right)\right] \\
&+ \int_{-b/2}^{+b/2} \frac{\gamma_v}{4\pi}\left(\frac{1}{2D + xv + xw}\right)\left[\frac{1}{2}\ln\left(\frac{16}{1-k^2}\right)\right] \\
&+ \int_{-b/2}^{+b/2} \frac{\gamma_v}{4\pi}\left(\frac{1}{2D + xv + xw}\right)\left[\frac{1}{8}\left(\ln\left(\frac{16}{1-k^2}\right) - 1\right)\left(1-k^2\right)\right]
\end{aligned}$$

But now look very closely at the first integral to be obtained. Recognize that

$$v_{xw} = \int_{-b/2}^{+b/2} \frac{\gamma_v}{4\pi}\left(\frac{1}{xv - xw}\right)$$

is nothing more than the classical fixed-wing problem presented in Part I of this note.

This is a key result that Glauert provided in his 1923 report because it says the so-called "near wake" of a U-turning fixed wing (i.e., think a rotor blade's near wake) is no tougher problem than the straight flying wing to which is added the influence of a curved "far wake." For the elliptical bound circulation used as the example in this note, the spanwise integration becomes

$$(0.39) \quad
\begin{aligned}
v_x = &\frac{\Gamma_o}{2b} \\
&+ \int_{-b/2}^{+b/2} \frac{\gamma_v}{4\pi}\left(\frac{1}{xv - xw}\right)\left[\frac{1}{4}\left(\ln\left(\frac{16}{1-k^2}\right) - \frac{1}{2}\right)\left(1-k^2\right)\right] \\
&+ \int_{-b/2}^{+b/2} \frac{\gamma_v}{4\pi}\left(\frac{1}{2D + xv + xw}\right)\left[\frac{1}{2}\ln\left(\frac{16}{1-k^2}\right)\right] \\
&+ \int_{-b/2}^{+b/2} \frac{\gamma_v}{4\pi}\left(\frac{1}{2D + xv + xw}\right)\left[\frac{1}{8}\left(\ln\left(\frac{16}{1-k^2}\right) - 1\right)\left(1-k^2\right)\right]
\end{aligned}$$

10

The additional three integrals can be grouped into one integral. But first, the vortex circulation strength, assuming an elliptical bound circulation for the wing lifting line, Eq. (0.8), is substituted into Eq. (0.39). Next the elliptic integral modulus, k^2, from Eq. (0.31), is substituted into Eq. (0.39). (I would have included the results of these substitutions, but the resulting expression is way too long.) Then a selection of wingspan stations, xw, is made (say 50) and, in short order, Mathcad calculated the induced velocity distributions at any turning distance, D.

Despite the appearance of possible singularities in Eq. (0.39), Mathcad actually experienced no numerical integration problems. I *did not* let Mathcad try to simplify the integrand. The temptation is to fiddle with $1\text{-}k^2$, which Mathcad or I fouled up. A very unproductive effort given Mathcad's speed on my Dell computer.

Glauert, in R & M 866, assumed that the turning radius was considerably greater than the wingspan, which allowed simple integration of Eq. (0.39), the result being Eq. (0.24). But consider the results as the wing makes tighter and tighter U-turns. A non-dimensional measure of the semicircle's tightness is wingspan, b, divided by the distance from the "pylon," D. The tightest turn would be when the port wingtip is touching the "pylon," in which case D = b/2 or b/D = 2.0. This corresponds to a rotor blade with zero root cutout. A turning ratio of b/D = 1 corresponds to a 0.33 root cutout. The extreme in the other direction would be, of course, not turning at all and so D = ∞ and b/D = 0.

For simple illustration purposes, let the wingspan be unity (i.e., b = 1.0 foot) and let the maximum elliptical bound circulation, which occurs at the wing mid-span, be two (i.e., Γ_o = 2.0 square feet per second). Thus, for the following examination, Γ_o /2b = 1.0 foot per second. Two results are immediately known from the preceding discussion:

Turn parameter, b/D	Spanwise induced velocity, v_x	Source
Not Turning	$v_x = \Gamma_o /2b = 1.0$	Eq. (0.1)
Wide Turn	$v_x = 1+xw/2D$	Eq. (0.24)

The results for several tighter and tighter turns are shown with Figures 4 through 7. For a turn distance D that is 10 times the wingspan, Glauert's approximation is very useful as Fig. 4 shows. When the turn distance is equal to the wingspan (equivalent to a rotor blade root cutout of 1/3), the distortion in induced velocity across the wingspan is significant, as shown with Fig. 5. This distortion grows more pronounced as the turn distance shrinks, which is illustrated by Figs. 6 and 7. These two figures correspond to a rotor blade root cutout of 0.1667 and 0.0476, respectively.

Now consider the numerical double integration involved in this U-turning wing problem. Figure 6 offers a virtually exact example to which numerical integration can be compared. The integration problem at hand is this:

$$(0.40) \quad v_{xw} = \int_{-b/2}^{+b/2} \int_{-\pi}^{0} \frac{\gamma_v}{4\pi} \left\{ \frac{(D+xv)(D+xw)\cos\theta - (D+xv)^2}{\left[(D+xv)^2 + (D+xw)^2 - 2(D+xv)(D+xw)\cos\theta \right]^{3/2}} \right\} d\theta\, dxv$$

Philosophically, Glauert found the fixed-wing induced velocity equation is buried obscurely within this U-turning wing problem. Therefore, the Mathcad-provided integration scheme will encounter all of the fixed-wing problems at the wingtips. (Mathcad returns the notice "will not converge," which makes for frustration.) A second thing you know is that the integrand's denominator can get very, very small or even be zero when $\theta = 0$. Both these probable problems suggest using the fixed-wing coordinate transformations, which to repeat, are

$$(0.41) \quad xv = -\frac{b}{2}\cos\beta \qquad dxv = \frac{b}{2}\sin\beta \qquad xw = -\frac{b}{2}\cos\alpha$$

and assume an elliptical bound circulation along the wing's lifting line so that

$$(0.42) \quad \gamma_v = -\Gamma_o \cos\beta\, d\beta$$

With the above thoughts in mind, a "brute force" numerical integration goes like this:

$\Gamma_o = 2 \qquad b = 1 \qquad D = 0.7$

Dimension integration.

Number of radial stations at which vortices leave wing, $M = 90$

Number of azimuthal stations between 0 and 180 degrees, $N = 18{,}000$

Range of radial stations where induced velocity is calculated, $s = 0,1\ldots\ldots M-1$

Then proceed with these calculations

$$\alpha_s = \frac{\pi}{M}\left(s + \frac{1}{2}\right)$$

$$n = 0,1\ldots\ldots N \qquad \theta_n = \left(-\frac{\pi}{N}\right)n$$

$$m = 0,1\ldots\ldots M \qquad \beta_m = \left(\frac{\pi}{M}\right)m$$

$$dvd\beta d\theta_{n,m} = \frac{\Gamma_o}{4\pi}\cos\beta_m \left\{ \frac{\left(D - \frac{b}{2}\cos\beta_m\right)\left(D - \frac{b}{2}\cos\alpha_s\right)\cos\theta_n - \left(D - \frac{b}{2}\cos\beta_m\right)^2}{\left[\left(D - \frac{b}{2}\cos\beta_m\right)^2 + \left(D - \frac{b}{2}\cos\alpha_s\right)^2 - 2\left(D - \frac{b}{2}\cos\beta_m\right)\left(D - \frac{b}{2}\cos\alpha_s\right)\cos\theta_n \right]^{3/2}} \right\}$$

$$dvd\beta_m = \frac{\pi}{N}\sum_{n=0}^{N-1} \frac{dvd\beta d\theta_{n,m} + dvd\beta d\theta_{n+1,m}}{2}$$

$$v_s = \frac{\pi}{M}\sum_{m=0}^{M-1} \frac{dvd\beta_m + dvd\beta_{m+1}}{2}$$

$$xw_s = -\frac{b}{2}\cos\alpha_s$$

The brute-force aspects of the above scheme are obvious. The wake age from θ = 0 to 180 degrees is divided into 18,000 segments or 0.01 of a degree. The spanwise segmentation is a little more rational. Ninety (90) vortices are trailed, and induced velocity at the wing is calculated in between each pair of trailed vortices. This density is far from practical for the real problems rotorcraft engineers are solving everyday—with today's computers. Calculating area as the sum of rectangular slivers is hardly advanced. Despite the obvious improvements that might be made, the scheme worked.

The first numerical integration result, compared to the virtually exact solution obtained by following Glauert, is shown with Fig. 8. The agreement over 99.9% of the wingspan is more than acceptable for engineering purposes. The only problem that occurred was calculation of induced velocity at the most outboard span station (i.e., s + 1/2 = 89.5 or xw = 0.4999238476). This span station is half way between the vortex trailed from the tip (i.e., m = 90) and the next vortex inboard at m = 89. The numerical solution gave v = 19.65 ft/sec versus the virtually exact 1.206 ft/sec. In contrast, the port wingtip encountered no such problems. Other than this one ridiculous answer at the starboard wingtip (plus being rather slow), the numerical integration scheme functioned in a satisfactory manner.

There are several interesting features to this U-turning wing problem. For example, the numerical integration proceeded from port to starboard wingtip with the numerous trailed vortices in between. Figure 9 illustrates what the induced-velocity wake age summation appears like for the calculation point next to the wing mid-span. The span station of interest is s + ½ (α_s = 90.5 degrees, xw = 0.0087). Figure 9 shows that dv/dβ sees the impending discontinuity at the span station point, but the summation averages the calculation to the left of the point with the calculation to the right of the point. Therefore, the induced velocity, the integral found from the

$$\text{induced velocity, } v = \text{area under} \frac{dv}{d\beta} \text{ versus } \beta$$

is obtained with quite reasonable results.

Another interesting behavior of this U-turning wing problem is shown with Fig. 10. This figure looks at the wake age integration involved with

$$\frac{dv}{d\beta} d\beta = \text{area under} \frac{d\left(\frac{dv}{d\beta} d\beta\right)}{d\theta} \text{ versus } \theta$$

The summation is illustrated at the two vortex trailed wing stations of β = 160 and β = 162 degrees (i.e., m = 80 and m = 81). The station at which induced velocity is sought is α_s = 161 degrees. The fascinating point made here is that the two vortices appear to make enormous contributions to induced velocity within the first 2 degrees of wake age. This is one of the reasons such small increments in wake age (i.e., 180 degrees of wake divided into 18,000 segments) are required for the rudimentary rectangular area summation scheme. The spanwise distribution of dv/dβ, provided with Fig. 11, shows just how large the numbers are that, when summed, however, come out v = 1.1968318858.

The situation near the port wingtip, which is closest to the pylon, is quite similar to that near the starboard wingtip. The conclusion is that the first 15 degrees of wake age must be very densely populated with points if a rudimentary numerical integration is used. Fortunately, advanced methods currently used in the rotorcraft industry accomplish the numerical integration much more efficiently.

Rotorcraft engineers have improved their non-uniform induced-velocity calculating methods by dividing the wake into a near wake and a far wake. Thus Fig. 8 shows that the near wake (i.e., $\theta = 0$ to -15 degrees in this case) gives the most trouble for numerical integration, particularly at the wingtips. The far wake (i.e., θ from -15 to $\theta = -180$ degrees in this case) responds to numerical integration with virtually no problems. In fact, the wake age can be divided into 1-degree segments versus 0.01-degree segments, and virtually the same contribution of the far wake to the induced velocity at the wing will be obtained.

The U-turning wing problem can be divided into a near wake and a far wake with relative ease. The induced velocity at the wing due to 180 degrees of circular arc wake in elliptic integral form is

$$(0.43) \quad v_{xw} = \int_{-b/2}^{+b/2} \frac{-\dfrac{\partial\Gamma}{\partial xv}}{4\pi} \left[\frac{\displaystyle\int_0^{\pi/2}\sqrt{1-k^2\sin^2\phi}\,d\phi}{xv-xw} + \frac{\displaystyle\int_0^{\pi/2}\frac{1}{\sqrt{1-k^2\sin^2\phi}}\,d\phi}{2D+xv+xw} \right] dxv$$

Keep in mind that $\phi = \pi/2$ is closest to the wing. Conversely, $\phi = 0$ corresponds to the end of the wake, or where the wing was *before* it started the U-turn. Therefore, the wake integration amounts to integrating from zero up to the start of the near wake, say ϕ_{NW}, and then adding the near-wake contribution, which extends from $\phi = \phi_{NW}$ to $\phi = \pi/2$. It is, however, much more direct in this case, to subtract from the total wake (i.e., $\int_0^{\pi/2} f(\phi)d\phi$) the wake behind the near wake (i.e., $\int_0^{\phi_{NW}} f(\phi)d\phi$). Thus, the two elliptic integrals are rearranged as follows:

$$(0.44)$$
$$\text{Near wake} = \int_0^{\pi/2}\sqrt{1-k^2\sin^2\phi}\,d\phi - \int_0^{\phi_{NW}}\sqrt{1-k^2\sin^2\phi}\,d\phi = \int_0^{\chi}\sqrt{1-k^2\sin^2\phi}\,d\phi - k^2\sin\phi_{NM}\sin\chi$$

$$\text{Near wake} = \int_0^{\pi/2}\frac{1}{\sqrt{1-k^2\sin^2\phi}}\,d\phi - \int_0^{\phi_{NW}}\frac{1}{\sqrt{1-k^2\sin^2\phi}}\,d\phi = \int_0^{\chi}\frac{1}{\sqrt{1-k^2\sin^2\phi}}\,d\phi$$

where the angle, χ, a new upper limit of integration, is given as

$$(0.45) \quad \chi = 2\arctan\left(\frac{\sqrt{1-k^2\sin^2\phi_{NW}} - \sin\phi_{NW}\sqrt{1-k^2}}{\cos\phi_{NW}} \right)$$

14

Then, in elliptic integral shorthand, the near-wake contribution to induced velocity at the wing is simply

$$(0.46) \quad \left(v_{xw}\right)^{Near}_{Wake} = \int_{-b/2}^{+b/2} \frac{-\dfrac{\partial \Gamma}{\partial xv}}{4\pi} \left[\frac{E(\chi,k)-k^2 \sin \phi_{NM} \sin \chi}{xv-xw} + \frac{F(\chi,k)}{2D+xv+xw} \right] dxv$$

where

$$E(\chi,k) = \int_0^\chi \sqrt{1-k^2 \sin^2 \phi}\, d\phi$$

$$(0.47)$$

$$F(\chi,k) = \int_0^\chi \frac{1}{\sqrt{1-k^2 \sin^2 \phi}}\, d\phi v$$

In like manner, the induced velocity at the wing due to the far wake becomes

$$(0.48) \quad \left(v_{xw}\right)^{Far}_{Wake} = \int_{-b/2}^{+b/2} \frac{-\dfrac{\partial \Gamma}{\partial xv}}{4\pi} \left[\frac{\int_0^{\phi_{NW}} \sqrt{1-k^2 \sin^2 \phi}\, d\phi}{xv-xw} + \frac{\int_0^{\phi_{NW}} \dfrac{1}{\sqrt{1-k^2 \sin^2 \phi}}\, d\phi}{2D+xv+xw} \right] dxv$$

where, to repeat, $k^2 = \dfrac{4(D+xw)(D+xv)}{(2D+xv+xw)^2}$

This completes the discussion of the U-turning wing problem. Two points have been made.

(1) A virtually exact calculation of induced velocity without numerical integration questions has been provided. Figure 6 gives an example to which any numerical integration result may be compared.

(2) The so-called near wake is built upon the fundamental integral solved by the fixed-wing community, which is

$$(0.49) \quad \text{Fixed Wing}\left(v_{xw}\right) = \int_{-b/2}^{+b/2} \frac{-\dfrac{\partial \Gamma}{\partial xv}}{4\pi} \left[\frac{1}{xv-xw} \right] dxv$$

II. The Wing Done With Rotor Notation

The next step along the bridge from the fixed-wing world to the rotary-wing world is to change to rotor blade geometry and notations. This geometry is provided with Fig. 12. The intent here is to think of a one-bladed rotor in hovering flight. (The case of forward flight begins in Part III of this note.) The rotating wing is again represented as a lifting line having an elliptical bound circulation. The trailing vortex wake structure resembles a lock washer or, perhaps more descriptively, a "slinky" spring-like toy. That is, each vortex will have a circular path just like the U-turning wing problem. The addition is that each trailing vortex spirals downward at a constant rate and the wake age can extend back to the beginning of time. In short, the wake of this rotating wing or, better yet, a one-bladed hovering rotor, need not stop at minus 180 degrees as was done with the U-turning wing.

Now study Figure 12's geometry quite closely. The rotor blade is shown rotating around the Z axis, which is positive down. The blade rotates in the X − Y plane where X is taken positive "forward," although what forward means in this case of no forward speed is not really meaningful. The Y axis is normal to the X − Z plane. This X, Y, Z axis system does not rotate with the blade, nor does it move with time.

The blade itself has a radius, R, measured from the Z axis. The blade is shown in Fig. 12 with a root cutout, r_c. Thus, the blade's span (thinking in terms of a wing) is simply R − r_c. Any radial station, measured positive outward from the Z axis and along the lifting line, is denoted by, r.

The blade's rotation angle is measured by the azimuth angle ψ, which, for convenience, equals zero when the blade lies along the negative X axis. The azimuth angle increases with time simply as the rotational speed Ω in radians per second times time in seconds. Obviously, Fig. 12 is a snapshot at any given time you care to start the watch. The blade is simply going round and round and the trailed vortex structure is left in space to descend at a prescribed rate, dZ/dt, in feet per second. Figure 12 is drawn to imply that the blade has been rotating for the time it takes to complete about two revolutions. However, the arrow head shown at the end of the one trailed vortex implies that time has been going on forever and, with a longer piece of paper, the spiral would extend down and around the Z axis to infinity.

As with the preceding fixed-wing examples, the Biot-Savart law requires a very careful mathematical definition for the blade and vortex wake dimensions. This is even truer when tackling the rotor blade problem. Using Fig. 12 as the geometric model of a single-bladed rotor, the radius station, r, at which the induced velocity is sought is set relative to the X − Y − Z axis by

(0.50) $Xr = -r \cos \psi$ $Yr = +r \sin \psi$ $Zr = 0$

A vortex trails aft from the blade from radius station rv. Any segment of this long spiraling vortex is therefore deposited at a point behind the blade and below the X − Y plane. This vortex segment, dS, is located at the coordinates

$$(0.51) \quad Xv = -rv\cos\theta \qquad\qquad Yv = +rv\sin\theta \qquad\qquad Zv = +\frac{dZv}{dt}\Delta t$$

Equation (0.51) introduces the possibility that the wake trailing behind the rotor blade does not stay in the $X-Y$ plane in which the rotor blade turns. This is quite different from classical fixed-wing wake geometry assumptions. The rotor-blade wake descends with some velocity, dZv/dt, and this velocity need not be constant. In fact, in the more complete analyses of rotor systems, freedom is given for any given vortex segment to wander throughout the $X-Y-Z$ axis system. For elementary discussion purposes, just assume a constant-diameter spiral (i.e., neither rv nor dZv/dt are influenced by time). Furthermore, it is not necessary at this point in the discussion to be more specific about the vortex segment's descent velocity.

Now as to the matter of time introduced by Eq. (0.51); for the rotor blade, the time increment, Δt, represents the time, t, it takes to travel back from the blade, which is at the snapshot azimuth angle, ψ, (at time, t_o) to the vortex segment, dS, which is located at θ (at time, t) . That is

$$(0.52) \quad \Delta t = t - t_o$$

Since the blade's angular rotation speed is Ω, it follows that

$$(0.53) \quad \Delta t = t - t_o = \frac{\theta - \psi}{\Omega}$$

which immediately says that

$$(0.54) \quad Zv = +\frac{dzv}{dt}\Delta t = \frac{dzv}{dt}\left(\frac{\theta - \psi}{\Omega}\right) = \frac{dzv}{\Omega dt}\theta = \frac{dzv}{d\theta}\theta$$

In many propeller studies, dZv/dθ is a measure of helix angle or sometimes propeller pitch.

Now, quite methodically, begin with the Biot-Savart law as previously stated:

$$(0.55) \quad d\left(dv_x / dxv\right) = \frac{\gamma_v}{4\pi}\left[\frac{L_i dS_j - L_j dS_i}{L^3}\right]d\theta$$

where the dimensions are expressed as vectors. The distance, L, between the vortex segment to the radius station, r, at which the induced velocity is sought, is determined by

$$L = L_i + L_j + L_k = (Xr - Xv)i + (Yr - Yv)j + (Zr - Zv)k$$

where $\quad Xr = -r\cos\psi \qquad\qquad Yr = +r\sin\psi \qquad\qquad Zr = 0$

$$(0.56)$$
$$\qquad Xv = -rv\cos\theta \qquad\qquad Yv = +rv\sin\theta \qquad\qquad Zv = +\frac{dzv}{d\theta}\theta$$

$$\text{and} \quad L^3 = \left[(Xr - Xv)^2 + (Yr - Yv)^3 + (Zr - Zv)^2\right]^{3/2}$$

In a similar manner, the vortex is described by

(0.57) $S = S_i + S_j + S_k = (Xv)\mathbf{i} + (Yv)\mathbf{j} + (Zv)\mathbf{k}$

but with rotor-blade vortex geometry,

$$dS_i = \frac{\partial S_i}{\partial \theta}d\theta = \frac{\partial Xv}{\partial \theta}d\theta = (rv\sin\theta)d\theta$$

(0.58) $$dS_j = \frac{\partial S_j}{\partial \theta}d\theta = \frac{\partial Yv}{\partial \theta}d\theta = (rv\cos\theta)d\theta$$

$$dS_k = \frac{\partial S_k}{\partial \theta}d\theta = \frac{\partial zv}{\partial \theta}\theta$$

The substitution of this rotor-blade geometry into the Biot-Savart law gives, with simplification

(0.59) $$d(dv_r / drv) = \frac{\gamma_v}{4\pi}\left\{\frac{rv^2 - r(rv)\cos(\psi - \theta)}{\left[rv^2 + r^2 - 2r(rv)\cos(\psi - \theta) + \left(\frac{dzv}{d\theta}\right)^2\theta^2\right]^{3/2}}\right\}d\theta$$

Because this is a single-bladed rotor in hover, there is an opportunity to choose the blade azimuth position at any value that is convenient. This is because the hover problem is completely symmetrical around the Z axis and "forward" has no meaning. (This is not possible in the forward flight case, as you will see in Part III of this note.) Given this latitude, choose $\psi = 0$. This reduces Eq. (0.59) to

(0.60) $$d(dv_r / drv) = \frac{\gamma_v}{4\pi}\left\{\frac{rv^2 - r(rv)\cos\theta}{\left[rv^2 + r^2 - 2r(rv)\cos\theta + \left(\frac{dzv}{d\theta}\right)^2\theta^2\right]^{3/2}}\right\}d\theta$$

which is a variation on Eq. (0.29) arrived at for the fixed wing after a U-turn. The variation is, of course, the addition of the term

$$\left(\frac{dzv}{d\theta}\right)^2\theta^2$$

Now let me address the wake age parameter, θ. The vortex wake leaves the blade lifting line referenced to $\psi = 0$. Therefore the smallest that θ can be is $\theta = \psi = 0$. The vortex spirals backwards (round and round and down) to $\theta = -\infty$. While it is not practical to go all the way back to $\theta = -\infty$, the intent is to go as far back as possible to avoid missing any influence of what many refer to as the far wake. Nevertheless, the integration over the wake age becomes

$$(0.61) \quad dv_r / drv = \int_{-\infty}^{0} \frac{\gamma_v}{4\pi} \left\{ \frac{rv^2 - r(rv)\cos\theta}{\left[rv^2 + r^2 - 2r(rv)\cos\theta + \left(\frac{dzv}{d\theta}\right)^2 \theta^2 \right]^{3/2}} \right\} d\theta$$

The immediate objective is to perform the integration required by Eq. (0.61). Suppose the vortex circulation, γ_v, does not vary with wake age. And suppose the vortex descent measure, $dzv/d\theta$, is constant. The only immediate numerical problem that is apparent in Eq. (0.61) is when the integrand's denominator is identically zero or so close to zero that numerical integration built into Mathcad flounders. This situation will *only* occur when θ is actually zero *and* when $r = rv$.

To illustrate the results of integrating Eq. (0.61) over the wake age using Mathcad's built-in scheme, choose some rational values for a single-bladed rotor. For this example

Parameter	Value
Rotor radius, R, feet	30.0
Root cutout, r_c, feet	3.0
Trail vortex from radius, rv, feet	27.0
Calculate induced velocity at radius, r, feet	16.5
Trailed vortex strength, γ_v, ft^2 per second	1,265.0
Vortex descent measure, $dzv/d\theta$, feet per radian	2.0
Wake age, θ_{end}, radians	−157.0
Number of 360-degree spirals	25
Distance from rotor down to last spiral, zv, feet	314

Mathcad was quite happy to whip out the answer so long as the input was chosen that avoids $r = rv$ by a considerable margin. (Just imagine the wake age integral in summation form with wake age segments of 0.01 degrees! It would take forever.) In the blink of an eye Mathcad produced Fig. 13. Figure 13 shows that induced velocity accumulates very quickly with increasing number of spirals included in the integration. Closer inspection of Fig. 14, an enlargement of Fig. 13, shows that the vortex segments included in the first half spiral contribute in a rather linear fashion to the induced velocity at blade radius station, r. But as the spiral continues around, it comes back underneath the blade (see Fig. 12) and the close proximity allows the vortex to become very influential. In short, the denominator in Eq. (0.61) with θ around −270 degrees is very influenced by the vortex descent measure, $dzv/d\theta$.

In advanced, modern numerical integration of the real rotor system problem, wandering vortices do come close and, indeed, even intersect the lifting line or lifting surface of the blade that trailed the vortices. That is to say Eq. (0.61)'s denominator finds some way to go to zero in the real problem. Furthermore, when there are more blades to consider, the ensuing possibilities of this denominator going to zero has been a major source of frustration in achieving accurate solutions for the rotor hovering and forward flight problems. The current crutch most widely used has been to add

20

what is called a vortex core to the denominator of Eq. (0.61) so zero can never occur. The fact that a vortex does have a real physical core of measurable diameter makes the core's inclusion in Eq. (0.61) reasonable. This concept of a vortex core diameter, VCD, means that Eq. (0.61) can be written as

$$(0.62) \quad dv_r / drv = \int_{-\infty}^{0} \frac{\gamma_v}{4\pi} \left\{ \frac{rv^2 - r(rv)\cos\theta}{\left[rv^2 + r^2 - 2r(rv)\cos\theta + \left(\frac{dzv}{d\theta}\right)^2 \theta^2 + VCD^2 \right]^{3/2}} \right\} d\theta$$

To make progress over recent years, technologists have achieved considerable numerical stability even when tackling the hardest problems using this concept of a vortex core. For this part of the note, completely dismiss the whole vortex core diameter issue.

Going on then, consider the collection of all the trailed vortices by performing the radial integration over the blade span from the root cutout, r_c, to the blade tip, $r = R$. This step begins by assuming a bound circulation distribution carried on the lifting line. Assume the bound circulation has an elliptical distribution[4] described by

$$(0.63) \quad \Gamma_r = \Gamma_o \sqrt{1 - \frac{(2r - r_c - R)^2}{(R - r_c)^2}}$$

which gives the circulation strength of a vortex trailing from radius station, rv, as

$$(0.64) \quad \gamma_v = -1 \left\{ \frac{-2R\Gamma_o}{\sqrt{1 - \frac{(2rv - r_c - R)^2}{(R - r_c)^2}}} \left[\frac{2rv - r_c - R}{(R - r_c)^2} \right] \right\} drv$$

The induced velocity along the blade's radius collecting all vortices is then

$$(0.65) \quad v_r = \int_{rc}^{R} \int_{-\infty}^{0} \frac{1}{4\pi} \frac{2\Gamma_o}{\sqrt{1 - \frac{(2rv - r_c - R)^2}{(R - r_c)^2}}} \left[\frac{2rv - r_c - R}{(R - r_c)^2} \right] \left\{ \frac{rv^2 - r(rv)\cos\theta}{\left[rv^2 + r^2 - 2r(rv)\cos\theta + \left(\frac{dzv}{d\theta}\right)^2 \theta^2 \right]^{3/2}} \right\} d\theta \, drv$$

Now, let me illustrate a completely numerical solution for this double integral.

---

[4] Keep in mind that the more general distribution used by fixed-wing engineers, Eq. (0.23), could be used to extend the results beyond an elliptical distribution.

21

Now, from Parts I and II of this note, the numerical integration of Eq. (0.65) will not converge to a solution because of any number of singular points. Mathcad's built-in integration scheme flounders even if a close-proximity situation occurs. You also know that the induced velocity—given an elliptical bound circulation along the lifting line—must contain the solution for a fixed wing. That is, at the very least

$$v_r = \frac{\Gamma_o}{2(R - r_c)}$$

The approach then is to first borrow the fixed-wing solution technique of letting

$$r = \left(\frac{R + r_c}{2}\right) - \left(\frac{R - r_c}{2}\right)\cos\alpha = a - b\cos\alpha$$

(0.66) $$rv = \left(\frac{R + r_c}{2}\right) - \left(\frac{R - r_c}{2}\right)\cos\beta = a - b\cos\beta$$

$$drv = \left(\frac{R - r_c}{2}\right)\sin\beta\,d\beta = b\sin\beta\,d\beta$$

where β goes from 0 to π. This coordinate system change at least transforms the vortex circulation strength, γ_v, of Eq. (0.64) to the very much simpler

(0.67) $$\gamma_v = -\Gamma_o \cos\beta\,d\beta$$

The completed substitution of Eqs. (0.66) and (0.67) into Eq. (0.65) restates the induced-velocity double integral problem as

(0.68)

$$v_r = \int_0^\pi \int_{-\infty}^0 \frac{-\Gamma_o \cos\beta}{4\pi}\left\{\frac{(a - b\cos\alpha)(a - b\cos\beta)\cos\theta - (a - b\cos\beta)^2}{\left[(a - b\cos\beta)^2 + (a - b\cos\alpha)^2 - 2(a - b\cos\alpha)(a - b\cos\beta)\cos\theta + \left(\frac{dzv}{d\theta}\right)^2\theta^2\right]^{3/2}}\right\}d\theta\,d\beta$$

So, now to numerically integrate Eq. (0.68). The scheme allows Mathcad to perform the wake age integral, *but* the spanwise integration is performed with a summation. This takes advantage of Mathcad's very, very fast integration over wake age. Thus, a useable numerical integration scheme reads like this:

22

INPUT

$\Gamma_o = 2$ $\qquad$ $R = 1.2$ $\qquad$ $r_c = 0.2$ $\qquad$ $\dfrac{dzv}{d\theta} = 0$

Dimension integration.

$\qquad$ Extent of wake age, $WA = -\pi$

$\qquad$ Number of radial stations at which vortices leave rotor blade, $M = 90$

$\qquad$ Range of radial stations where induced velocity is calculated, $s = 0,1.......M-1$

Then proceed with these calculations

$a = \dfrac{R - r_c}{2}$ $\qquad\qquad$ $b = \dfrac{R + r_c}{2}$

$\alpha_s = \dfrac{\pi}{M}\left(s + \dfrac{1}{2}\right)$

$m = 0,1......M$ $\qquad$ $\beta_m = \left(\dfrac{\pi}{M}\right)m$

$$dvd\beta_m = \int_{WA}^{0} \dfrac{-\Gamma_o \cos\beta}{4\pi}\left\{\dfrac{(a - b\cos\alpha)(a - b\cos\beta)\cos\theta - (a - b\cos\beta)^2}{\left[(a - b\cos\beta)^2 + (a - b\cos\alpha)^2 - 2(a - b\cos\alpha)(a - b\cos\beta)\cos\theta + \left(\dfrac{dzv}{d\theta}\right)^2 \theta^2\right]^{3/2}}\right\}d\theta$$

$v_s = \dfrac{\pi}{M}\sum_{m=0}^{M-1}\dfrac{dvd\beta_m + dvd\beta_{m+1}}{2}$

$r_s = a - b\cos\alpha_s$

Notice on this sample input that it corresponds to the U-turning wing problem of $D = 0.7$, $b = 1$, $\Gamma_o = 2$, which gives the induced velocity distribution shown on Fig. 8. This check case did check. Mathcad was faster and more accurate with the wake age integral broken into several ranges. The following seemed best

$$\int_{WA}^{0} f(\alpha,\beta)d\theta = \int_{-\frac{\pi}{180}5}^{0} f(\alpha,\beta)d\theta + \int_{-\pi}^{-\frac{\pi}{180}5} f(\alpha,\beta)d\theta + \int_{-3\pi}^{-\pi} f(\alpha,\beta)d\theta + \int_{WA}^{-3\pi} f(\alpha,\beta)d\theta$$

$\qquad$ Now consider a practical case of a 4-bladed, 44-foot-diameter rotor lifting about 10,800 pounds while operating at a tip speed, $V_t = \Omega R = 600$ ft/sec. The above input requires an estimate for maximum bound circulation, Γ_o, and the vortex segment descent rate, $dzv/d\theta$. Rational estimates for both parameters can be obtained. To begin with, assume each blade has a root cutout of $r_c = R/6$ and each blade has an elliptical bound circulation over its span. The bound circulation's maximum will be $\Gamma_o = 225$ ft^2/sec, which is calculated from

(0.69) $\qquad$ Lift per blade $= \dfrac{\pi}{8}\rho R V_t \Gamma_o\left[1 - \left(\dfrac{rc}{R}\right)^2\right]$ $\qquad$ so $\qquad$ $\Gamma_o = \dfrac{8L}{\pi\rho R V_t\left[1 - (rc/R)^2\right]}$

23

Next, assume a vortex segment, dS, is carried downward with the downwash velocity. From simple momentum theory, this downwash or induced velocity is 19.3 ft/sec when calculated with

(0.70) $\text{Momentum induced velocity} \equiv v_i = \sqrt{\dfrac{L}{2\rho\pi R^2}}$

Then, in one second, a segment will have descended 19.3 feet. But in one second, the rotor blade will move through a wake age angle of $\theta = \Omega$ times one second. Therefore, the vortex segment descent rate is simply

(0.71) $\dfrac{dzv}{d\theta} = \dfrac{v_i \text{ times 1 second}}{\Omega \text{ times 1 second}} = \dfrac{v_i}{V_t/R} = R\dfrac{v_i}{V_t}$

which is roughly 0.7 feet per radian for this representative example. This means that in one complete spiral revolution, the vertical distance will be $0.7(2\pi)$ feet or roughly 4.4 feet for every revolution. This is a measure of Fig. 12's spiral spacing or pitch.

To summarize this typical one-bladed rotor's operating situation, the representative calculations that follow were based on

INPUT

$\Gamma_o = 225\,\text{ft}^2/\text{sec}$ $R = 22\,\text{ft}$ $r_c = R/6$ $\dfrac{dzv}{d\theta} = 0.7\ \text{ft}/\text{rad}$

Dimension integration.

      Extent of wake age, WA = variable for this example

      Number of radial stations at which vortices leave rotor blade, M = 90

      Range of radial stations where induced velocity is calculated, $s = 0,1.......M-1$

An immediate question is: How many spirals does it take to accurately approximate an infinite wake? As seen from Fig. 15, perhaps about one hundred, 360-degree spirals captures the problem in a promising way. This amounts to 440 feet of wake or about 10 rotor diameters. A more quantitative measure of a practical engineering solution is induced horsepower, HP_i. This major contributor to total power is calculated as

(0.72) $HP_i = \dfrac{1}{550}\int_{rc}^{R} v_r dL_r = \dfrac{1}{550}\int_{rc}^{R} v_r\left(\rho V_r \Gamma_r\right) dr$

The calculation was made using the summation of 90 rectangular slivers. The results, tabulated below, indicate that even 20 spirals will neglect about 2 to 3 horsepower, which is on the order of 2 to 3 percent missing horsepower because the wake age was not extended to infinity. The ratio of calculated induced horsepower to ideal momentum horsepower (i.e., $Lv_i/550 = 95.524$ horsepower) is the fourth column in the table. The reciprocal of this ratio, known as Figure of Merit, is provided by the sixth column. A Figure of Merit above 1.0 is not possible and thus at least 10.5 spirals are required before a rational answer starts to become apparent. Clearly, an elliptical bound circulation,

24

which is ideal for a fixed wing (i.e., the equivalent of FM = 1 for a rotating wing), is far from ideal for a rotating wing.

Number of Spirals	Blade Lift	Calculated Induced HP	Ideal Induced HP	Calculated HP/HP_{ideal}	Figure of Merit
0.5	2712.52	29.57	95.52	0.31	3.23
1.5		55.31		0.58	1.73
2.5		70.41		0.74	1.36
3.5		80.32		0.8408	1.189
5.5		92.33		0.9666	1.0346
10.5		104.44		1.0934	0.9146
20.5		110.25		1.1541	0.8665
100.5		112.79		1.1808	0.8469
200.5		112.84		1.1813	0.8465

Do not assume that this example has provided anything more than a crude estimate for a single-bladed rotor's actual performance. The prescribed wake geometry used is very, very far from the wake visually observed in any number of experiments. The example would surely come out differently—and more accurately compared to experiment—if (or when) this sample problem is calculated with advanced methods in use today.

For the sake of completeness, Fig. 16 gives the running lift, ΔL_r, and running horsepower, ΔHP_i, versus radius station. These data are for 100.5 spirals.

This concludes Part I and Part II of this note. The next step is to apply this background to the single-bladed rotor in forward flight.

III. A Rotating Blade in Forward Flight

The next step in the bridge between a fixed and rotating wing is examined with this portion of the note. The rotating wing in forward flight deposits a rather complicated vortex wake in space as it flies away. A hint of the wake's complexity is seen below.
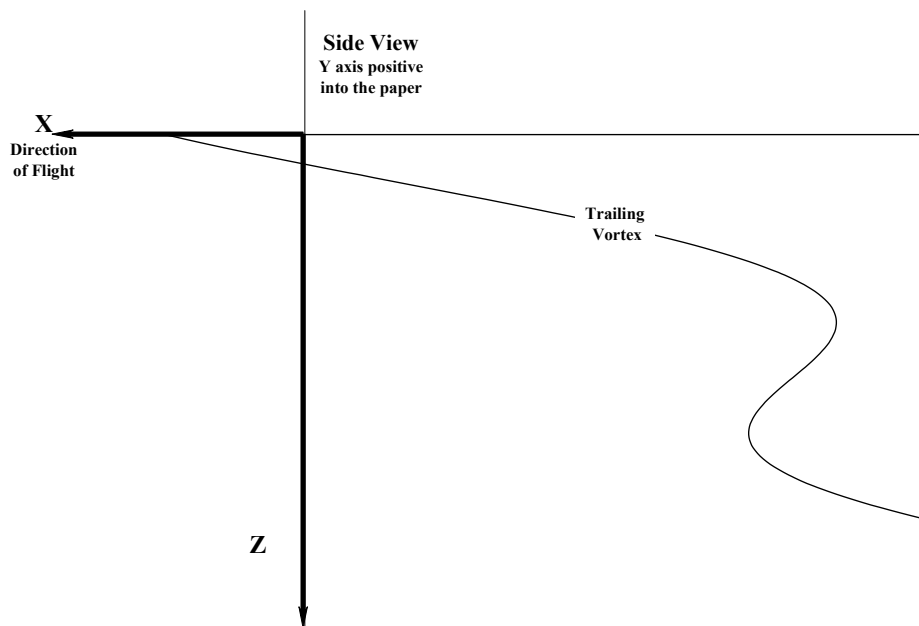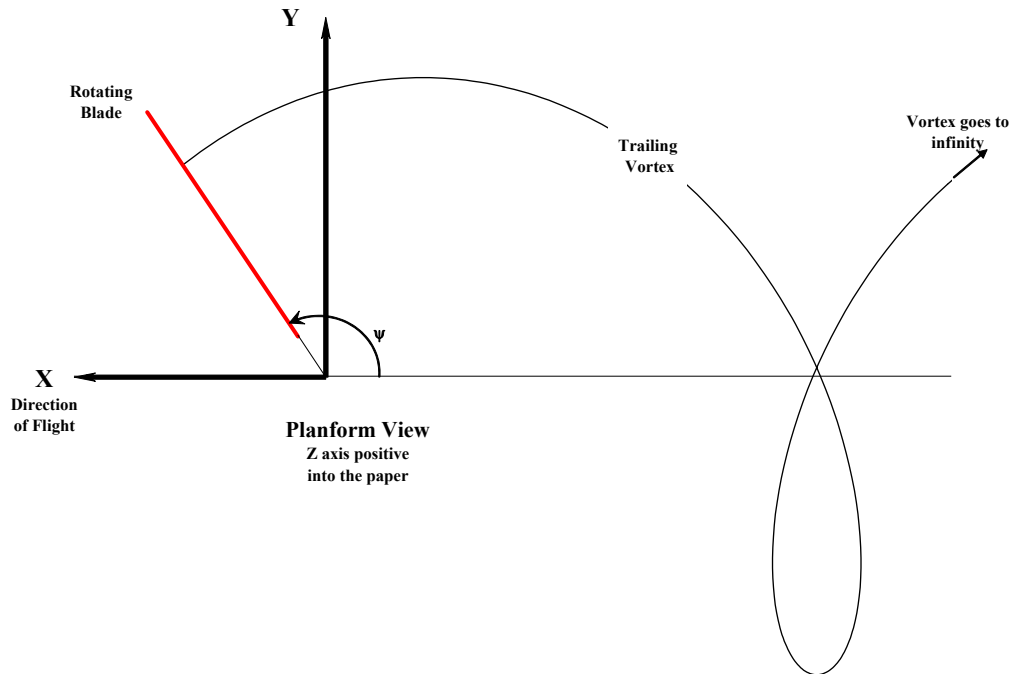
In the sketch (pg. 27), the rotating wing—the single-bladed rotor—is rotating about the Z axis in the X – Y plane at angular velocity, Ω, in radians per second. The blade is attached to a hub. The hub is located at X=Y=Z=0. The X – Y – Z axis system moves through space straight along the plus X direction with forward velocity, V, in feet per second. The axis system neither pitches nor rolls and it does not climb or descend. The rotor blade has a radius, R, in feet and a root cutout, r_c, in feet. The tip speed of the rotor is $V_t = \Omega R$ in feet per second. The one vortex shown illustrates the drifting-down, spiraling path typical of all vortices.

A more complete picture of the wake complexity is provided with Figs. 17 through 20. These figures have been drawn for an advance ratio, $\mu = V/V_t = 0.5$, and show the planform view. Start with Fig. 17 where the blade is at the azimuth angle, ψ, of 90 degrees. This azimuth is generally referred to as the advancing side of the rotor disc. In the fixed-wing problem, all vortices trail straight back, parallel to the X axis. Obviously, this is not true for a rotor blade. The tip vortex traces out a prolate cycloid, while the root cutout vortex follows a curtate cycloid. Figure 18 shows the planform view with the blade at the 180-degree azimuth position. Figure 19 places the blade at $\psi = 270$ degrees, which is the retreating side of the rotor disc. Notice that the two outboard vortices trailed from the blade sharply turn nearly back on the blade itself. Finally, Fig. 20 shows the blade at its most downwind position of $\psi = 360$ or zero degrees. Here the trailed vortices really attack the blade. The possibilities of any given vortex directly intersecting the generating lifting line are quite real in the practical problem.

Before bringing the Biot-Savart law to bear on this problem, there are a few aspects of the notations to observe. To begin with, rather than deal with the geometry dimensionally, use the conventional rotor non-dimensional notations of

(0.73)

$$x = \frac{r}{R} \quad \text{radius station where induced velocity is sought}$$

$$xv = \frac{r_v}{R} \quad \text{radius station where vortex is trailed}$$

$$\alpha_{tpp} \equiv \quad \text{angle of attack of the tip path plane, positive nose up}$$

$$\mu = \frac{V}{V_t} \cos\alpha_{tpp} \quad \text{advance ratio}$$

$$v_i \equiv \text{induced velocity calculated by momentum theory}$$

$$\lambda_{tpp} = \frac{V\sin\alpha_{tpp} - v_i}{V_t} \quad \text{inflow ratio}$$

Now, using Fig. 21 as the reference, methodically begin with the Biot-Savart law as previously stated:

(0.74) $\quad d(dv_x / dxv) = \frac{\gamma_v}{4\pi}\left[\frac{L_i dS_j - L_j dS_i}{L^3}\right]d\theta$

28

where the dimensions are expressed as vectors as displayed on Fig. 21. For the distance, L, between the vortex segment, dS, to the radius station, x, at which the induced velocity is sought, you have

$$L = L_i + L_j + L_k = (Xr - Xv)i + (Yr - Yv)j + (Zr - Zv)k$$

$$\text{where} \quad Xr = -R[x\cos\psi] \qquad\qquad Yr = +R[x\sin\psi] \qquad Zr = 0$$

(0.75)

$$Xv = -R[xv\cos\theta + \mu(\psi - \theta)] \qquad Yv = +R[xv\sin\theta] \qquad Zv = -R\lambda_{tpp}(\psi - \theta)$$

$$\text{and} \quad L^3 = \left[(Xr - Xv)^2 + (Yr - Yv)^3 + (Zr - Zv)^2\right]^{3/2}$$

In a similar manner, the vortex is described by

$$(0.76) \quad S = S_i + S_j + S_k = (Xv)i + (Yv)j + (Zv)k$$

but with rotor-blade vortex geometry, you have

$$dS_i = \frac{\partial S_i}{\partial\theta}d\theta = \frac{\partial Xv}{\partial\theta}d\theta = +R(xv\sin\theta + \mu\theta)d\theta$$

$$(0.77) \quad dS_j = \frac{\partial S_j}{\partial\theta}d\theta = \frac{\partial Yv}{\partial\theta}d\theta = +R(xv\cos\theta)d\theta$$

$$dS_k = \frac{\partial S_k}{\partial\theta}d\theta = +R\,\lambda_{tpp}\theta$$

The substitution of this rotor-blade and wake geometry into the Biot-Savart law gives, with simplification

(0.78)

$$\left[\frac{L_i dS_j - L_j dS_i}{L^3}\right] = \frac{xv^2 - x(xv)\cos(\psi - \theta) + \mu[xv\sin\theta - x\sin\psi + xv(\psi - \theta)\cos\theta]}{R\left\{\left[xv^2 + x^2 - 2x(xv)\cos(\psi - \theta)\right] + 2\mu(xv\cos\theta - x\cos\psi)(\psi - \theta) + (\psi - \theta)^2(\mu^2 + \lambda_{tpp}^2)\right\}^{\frac{3}{2}}}$$

As an intermediate step, integrate the Biot-Savart with respect to wake age assuming the vortex circulation is simply a constant. That is, tackle

$$(0.79) \quad (dv_x / dxv)_\psi = \frac{\gamma_v}{4\pi}\int_{-\infty}^{\psi}\left[\frac{L_i dS_j - L_j dS_i}{L^3}\right]d\theta$$

The purpose of this step was to test Mathcad's built-in integrator and be sure it did not flounder at any azimuth, ψ, or radius station, x, with the provision that $x \neq xv$. To perform this test, I set $\gamma_v = 4\pi$, and R = 1. I found that the near wake needed integration in several parts and finally selected integration as follows:

$$(0.80) \quad \int_{-\infty}^{\psi} \left[\frac{L_i dS_j - L_j dS_i}{L^3} \right] d\theta = \int_{\psi - \frac{\pi}{180}1}^{\psi} + \int_{\psi - \frac{\pi}{180}2}^{\psi - \frac{\pi}{180}1} + \int_{\psi - \frac{\pi}{180}5}^{\psi - \frac{\pi}{180}2} + \int_{\psi - \frac{\pi}{180}15}^{\psi - \frac{\pi}{180}5} + \int_{\psi - \frac{\pi}{180}90}^{\psi - \frac{\pi}{180}15} +$$

$$\int_{\psi - \frac{\pi}{180}180}^{\psi - \frac{\pi}{180}90} + \int_{-5\pi}^{\psi - \pi} + \int_{-20\pi}^{-5\pi}$$

Mathcad's built-in integrator struggled with the calculation at and near the blade's root end (i.e., around the root cutout region) in the azimuth region from ψ = 330 to 360 degrees. The reason for this struggle is, of course, the near-zero value of L, as Fig. 20 clearly shows. Adding a vortex core diameter would obviate the problem in regions where the vortices are so closely packed.

The next step requires picking a bound circulation for the blade's lifting line. Suppose the elliptical distribution is chosen and this distribution does not vary with azimuth. This means there will only be trailed vortices and no shed vortices to add to the problem for this example. (The case of a shed wake will be addressed shortly.) Thus,

$$(0.81) \quad \Gamma_{x,\psi} = \Gamma_o \sqrt{1 - \frac{(2x - x_c - 1)^2}{(1 - x_c)^2}} \qquad \text{does not vary with azimuth, } \psi$$

Then, borrowing from the fixed-wing solution technique, let

$$x = \frac{r}{R} = \left(\frac{1 + x_c}{2} \right) - \left(\frac{1 - x_c}{2} \right) \cos \alpha = a - b \cos \alpha$$

$$(0.82) \quad xv = \frac{r_v}{R} = \left(\frac{1 + x_c}{2} \right) - \left(\frac{1 - x_c}{2} \right) \cos \beta = a - b \cos \beta$$

$$dxv = \left(\frac{1 - x_c}{2} \right) \sin \beta \, d\beta = b \sin \beta \, d\beta$$

where β goes from 0 to π. This coordinate-system change at least transforms the trailed vortex circulation strength, γ_v, to the very much simpler

$$(0.83) \quad \gamma_v = -\Gamma_o \cos \beta \, d\beta$$

and thus the induced-velocity double integral problem for an elliptical bound circulation that does not vary with azimuth is restated as

$$(0.84)$$

$$v_r = \int_0^\pi \int_{-\infty}^\psi \frac{-\Gamma_o \cos \beta}{4\pi R} \left\{ \frac{xv^2 - x(xv)\cos(\psi - \theta) + \mu[xv \sin\theta - x\sin\psi + xv(\psi - \theta)\cos\theta]}{\left\{ [xv^2 + x^2 - 2x(xv)\cos(\psi - \theta)] + 2\mu(xv\cos\theta - x\cos\psi)(\psi - \theta) + (\psi - \theta)^2 (\mu^2 + \lambda_{tpp}^2) \right\}^{\frac{3}{2}}} \right\} d\theta \, d\beta$$

The question now arises as to what value of the maximum bound circulation, Γ_o, is representative for this example. The calculation of this single-bladed rotor's *average* or *steady* lift follows as:

$$dL_{r,\psi} = \rho\left(\vec{V}_{r,\psi} \times \vec{\Gamma}_{r,\psi}\right)dr \qquad \text{both V and } \Gamma \text{ are vectors}$$

$$dL_{x,\psi} = \rho V_{x,\psi}\Gamma_{x,\psi} \; Rdx = \rho\left[V_t\left(x+\mu\sin\psi\right)\right]\left[\Gamma_o\sqrt{1-\frac{\left(2x-x_c-1\right)^2}{\left(1-x_c\right)^2}}\,\right]Rdx$$

(0.85)
$$L_\psi = \int_{x_c}^1 dL_{x,\psi} = \int_{x_c}^1 \rho\left[V_t\left(x+\mu\sin\psi\right)\right]\left[\Gamma_o\sqrt{1-\frac{\left(2x-x_c-1\right)^2}{\left(1-x_c\right)^2}}\,\right]Rdx$$

$$L_\psi = \frac{\pi}{8}\rho R V_t\Gamma_o\left(1-x_c\right)\left(1+2\mu\sin\psi+x_c\right)$$

$$L_{steady} = \frac{1}{2\pi}\int_0^{2\pi}L_\psi\,d\psi = \frac{1}{2\pi}\int_0^{2\pi}\frac{\pi}{8}\rho R V_t\Gamma_o\left(1-x_c\right)\left(1+2\mu\sin\psi+x_c\right)d\psi$$

$$\text{Steady Lift per blade} = \frac{\pi}{8}\rho R V_t\Gamma_o\left[1-x_c^2\right] \qquad \text{so} \qquad \Gamma_o = \frac{8L_{Steady}}{\pi\rho R V_t\left[1-x_c^2\right]}$$

On this basis, choose the blade geometry from Part II

$$R = 22 \text{ feet}$$
$$x_c = 1/6 \text{ non-dimensional}$$

and the forward flight conditions for this Part III problem are:

$$\rho = 0.002378 \text{ slugs per cubic feet}$$
$$V_t = 603.605 \text{ feet per second}$$
$$\mu = 0.5 \text{ non-dimensional}$$
$$\lambda_{tpp} = -0.03 \text{ non-dimensional}$$
$$\Gamma_o = 225 \text{ square feet per second}$$

in which case the steady lift per blade is 2,712 pounds at 178 knots.

With this information as input, Mathcad and its built-in integrator is used to calculate Eq. (0.84) as follows:

INPUT

$\mu = 0.5$ $\qquad$ $\Gamma_o = 225$ $\qquad$ $R = 22$ $\qquad$ $x_c = 1/6$ $\qquad$ $\lambda_{tpp} = -0.03$

Dimension integration.

$\qquad$ Select azimuth station, ψ = variable for this problem

$\qquad$ Extent of wake age, $WA = -20\pi$

$\qquad$ Number of radial stations at which vortices leave rotor blade, $M = 90$

$\qquad$ Range of radial stations where induced velocity is calculated, $s = 0,1.......M-1$

Then proceed with these calculations

$$a = \frac{1-x_c}{2} \qquad\qquad b = \frac{1+x_c}{2}$$

$$\alpha_s = \frac{\pi}{M}\left(s + \frac{1}{2}\right)$$

$$x_s = \frac{r}{R} = \left(\frac{1+x_c}{2}\right) - \left(\frac{1-x_c}{2}\right)\cos\alpha_s = a - b\cos\alpha_s$$

$$m = 0,1......M \qquad\qquad \beta_m = \left(\frac{\pi}{M}\right)m$$

$$xv_m = \frac{r_v}{R} = \left(\frac{1+x_c}{2}\right) - \left(\frac{1-x_c}{2}\right)\cos\beta_m = a - b\cos\beta_m$$

$$dvd\beta_{s,m} = \int_{WA}^{\psi} \frac{-\Gamma_o \cos\beta}{4\pi R}\left\{ \frac{xv^2 - x(xv)\cos(\psi-\theta) + \mu\left[xv\sin\theta - x\sin\psi + xv(\psi-\theta)\cos\theta\right]}{\left\{\left[xv^2 + x^2 - 2x(xv)\cos(\psi-\theta)\right] + 2\mu(xv\cos\theta - x\cos\psi)(\psi-\theta) + (\psi-\theta)^2\left(\mu^2 + \lambda_{tpp}^2\right)\right\}^{\frac{3}{2}}} \right\} d\theta$$

$$v_{s,\psi} = \frac{\pi}{M}\sum_{m=0}^{M-1}\frac{dvd\beta_{s,m} + dvd\beta_{s,m+1}}{2}$$

$$x_s = a - b\cos\alpha_s$$

$\qquad$ The calculation of induced velocity at the lifting line—as created by the trailed vortices from the lifting line—now follows from the above scheme. Additionally, lift and horsepower distributions are calculated from

$$\Delta L_{s,\psi} = \left[\rho V_t\left(x_s + \mu\sin\psi\right)R\right]\left\{\Gamma_o\sqrt{1 - \frac{(2x_s - x_c - 1)^2}{(1-x_c)^2}}\right\}\Delta_s \Rightarrow \text{Running Lift}$$

$$L_\psi = \sum_{s=0}^{M-1}\Delta L_{s,\psi} \Rightarrow \text{Single-blade lift at input azimuth}$$

(0.86)

$$\Delta HP_{s,\psi} = \frac{1}{550}v_{s,\psi}\Delta L_{s,\psi} \Rightarrow \text{Running Horsepower}$$

$$HP_\psi = \sum_{s=0}^{M-1}\Delta HP_{s,\psi} \Rightarrow \text{Single-blade Horsepower at input azimuth}$$

$$\text{where } \Delta_s = \left(\frac{1+x_c}{2}\right)\left[\cos\left(\frac{\pi}{M}s\right) - \cos\left(\frac{\pi}{M}(s+1)\right)\right]$$

32

A representative illustration of azimuth varying induced velocity at several radial stations is shown on Figs. 22 and 23. Remember that this result is for a single-bladed rotor lifting 2,712 pounds at 0.5 advance ratio (i.e., V = 178 knots at V_t = 603.6 fps). Even more interesting is the azimuthal variation of the blade's total lift and induced horsepower, shown on Fig. 24. The average or steady induced horsepower is obtained by

$$(0.87) \quad \text{Steady Induced Horsepower} \equiv \text{HP}_i = \frac{1}{2\pi} \int_0^{2\pi} \text{HP}_\psi$$

The result is HP_i = 50.1 hp. This induced horsepower, calculated with the prescribed wake, compares to the ideal induced horsepower calculated in Part I as

$$(0.88) \quad \text{Ideal Induced Horsepower} \equiv \text{Ideal HP}_i \approx \frac{1}{550} (\text{Lift}) \left(\frac{\text{Lift}}{2\rho\pi R^2 V} \right) \quad \text{for} \quad \mu > 0.2$$

which yields ideal HP_i = 6.13 hp. This means that the elliptically loaded, single-bladed rotor requires about 8 times the power calculated by simple momentum theory!

An additional point made by Fig. 24 is that the highest lift is carried primarily on the advancing side of the rotor disc. As such, the rotor is out of trim because of the rolling moment inferred by Fig. 24.

This leads to the question: If the rotor has an elliptical bound circulation that varies with azimuth so that the rolling moment is zero, what is the induced power? And this leads to the fourth and final Part of this note.

IV. A Rotating Blade in Forward Flight With Zero Rolling Moment

The last step in the bridge between a fixed and rotating wing is concluded with this portion of the note. A fixed wing generally flies with zero rolling moment, RM. This same criterion can be applied to a rotating wing. [I refer to a rotating wing with RM = 0 as a "balanced" rotor.] Suppose the bound circulation of the single-bladed rotor is described by

$$(0.89) \quad \Gamma_{x,\psi} = (\Gamma_o + \Gamma_1 \sin \psi) \sqrt{1 - \frac{(2x - x_c - 1)^2}{(1 - x_c)^2}}$$

In this case the lift and rolling moment are found as

$$(0.90) \quad \begin{aligned} L_{Steady} &= \frac{\pi}{8} \rho R V_t \Gamma_o [1 - x_c] [(1 + x_c) \Gamma_o + \mu \Gamma_1] \\ RM_{Steady} &= -\frac{\pi}{128} \rho R^2 V_t \Gamma_o [1 - x_c] [8\mu(1 + x_c)\Gamma_o + (5 + 6x_c + 5x_c^2)\Gamma_1] \end{aligned}$$

and if the rolling moment is set to zero

$$(0.91) \quad \begin{aligned} \Gamma_1 &= -\frac{8\mu(1 + x_c)\Gamma_o}{(5 + 6x_c + 5x_c^2)} \\ L_{Steady} &= \frac{\pi}{8} \rho R V_t \Gamma_o [1 - x_c^2] \left[1 - \frac{8\mu^2}{(5 + 6x_c + 5x_c^2)} \right] \Gamma_o \end{aligned}$$

The Biot-Savart law of Eq. (0.84) now must include the trailed vortex circulation, γ_v, which is azimuth varying according to Eq. (0.89). Therefore, for this Part IV of the note:

$$(0.92)$$

$$v_{x,\psi} = \int_0^\pi \int_{-\infty}^\psi \frac{-(\Gamma_o + \Gamma_1 \sin \psi) \cos \beta}{4\pi R} \left\{ \frac{xv^2 - x(xv)\cos(\psi - \theta) + \mu[xv \sin\theta - x \sin\psi + xv(\psi - \theta)\cos\theta]}{\left\{ [xv^2 + x^2 - 2x(xv)\cos(\psi - \theta)] + 2\mu(xv\cos\theta - x\cos\psi)(\psi - \theta) + (\psi - \theta)^2 (\mu^2 + \lambda_{tpp}^2) \right\}^{\frac{3}{2}}} \right\} d\theta \, d\beta$$

The numerical integration of this slightly different equation (i.e., with azimuth varying circulation) follows exactly that given in Part III of this note.

The contribution of *trailed vorticity* to induced velocity at the lifting line of this "balanced" rotor is shown in Figs. 25 and 26. The total blade's lift and induced power is given with Fig. 27. These results are for the balanced rotor producing 2,712 pounds of lift at 178 knots and can be compared to Fig. 24, which is for the "unbalanced" rotor. Only trailed vortices are contributing to the induced power at this point. The additional induced velocity and horsepower due to the *shed wake* are still to be included.

A numerical solution scheme for the shed wake is relatively simple compared to that for the trailed wake. However, in the shed-wake problem, the vortex left behind the blade has a radial geometry and circulation just like the blade's when the blade was at that azimuth. However, the vortex circulation is the negative of the blade's bound circulation when it was there. The geometry of this shed-wake problem is shown on Fig. 28. Again, the conventional rotor non-dimensional notations are:

$$x = \frac{r}{R} \quad \text{radius station where induced velocity is sought}$$

$$xv = \frac{r_v}{R} \quad \text{radius station where vortex is trailed}$$

$$\alpha_{tpp} \equiv \quad \text{angle of attack of the tip path plane, positive nose up}$$

(0.93)

$$\mu = \frac{V}{V_t}\cos\alpha_{tpp} \quad \text{advance ratio}$$

$$v_i \equiv \quad \text{induced velocity calculated by momentum theory}$$

$$\lambda_{tpp} = \frac{V\sin\alpha_{tpp} - v_i}{V_t} \quad \text{inflow ratio}$$

Now, using Fig. 28 as the reference, begin with the Biot-Savart law

(0.94) $\quad d\left(dv_x / dxv\right) = \frac{\gamma_v}{4\pi}\left[\frac{L_i dS_j - L_j dS_i}{L^3}\right]d\theta$

where the dimensions are expressed as vectors as displayed on Fig. 28. The distance, L, between the shed-vortex segment, dS, to the radius station, x, at which the induced velocity is sought, is

(0.95)
$L = L_i + L_j + L_k = (Xr - Xv)i + (Yr - Yv)j + (Zr - Zv)k$

where $\quad Xr = -R[x\cos\psi] \qquad\qquad Yr = +R[x\sin\psi] \qquad Zr = 0$

$\qquad\quad Xv = -R[xv\cos\theta + \mu(\psi - \theta)] \qquad Yv = +R[xv\sin\theta] \qquad Zv = -R\lambda_{tpp}(\psi - \theta)$

and $\quad L^3 = \left[(Xr - Xv)^2 + (Yr - Yv)^3 + (Zr - Zv)^2\right]^{3/2}$

so $\quad L^3 = R\left\{\left[xv^2 + x^2 - 2x(xv)\cos(\psi - \theta)\right] + 2\mu(xv\cos\theta - x\cos\psi)(\psi - \theta) + (\psi - \theta)^2\left(\mu^2 + \lambda_{tpp}^2\right)\right\}^{\frac{3}{2}}$

Notice that the length, L, is the same for the shed wake as for the trailed wake. To continue then, the vortex element is described by

(0.96) $\quad S = S_i + S_j + S_k = (Xv)i + (Yv)j + (Zv)k$

but with rotor-blade shed-vortex geometry, the vortex extends radially and so the partial derivatives of S are with respect to xv. Thus

36

$$dS_i = \frac{\partial S_i}{\partial xv} dxv = \frac{\partial Xv}{\partial xv} dxv = -R\cos\theta\, dxv$$

(0.97) $$dS_j = \frac{\partial S_j}{\partial xv} dxv = \frac{\partial Yv}{\partial xv} dxv = +R\sin\theta\, dxv$$

$$dS_k = \frac{\partial S_k}{\partial xv} dxv = \frac{\partial Zv}{\partial xv} dxv = 0$$

With this information, the geometric part of the Biot-Savart law becomes

(0.98) $$\left[\frac{L_i dS_j - L_j dS_i}{L^3}\right] = \left\{-\frac{x\sin(\psi-\theta)+\mu(\psi-\theta)\sin\theta}{L^3}\right\} dxv$$

The Biot-Savart also needs the shed-vortex circulation as it varies with wake age. Thus,

(0.99)   Shed $$\gamma_v = -\left(\frac{d\Gamma_{x,\psi}}{d\psi}\right)_{\substack{at\ \psi=\theta \\ and \\ x=xv}} d\theta = -(\Gamma_1\cos\theta)\sqrt{1-\frac{(2xv-x_c-1)^2}{(1-x_c)^2}}\, d\theta$$

and the double integral giving induced velocity at any radius station, x, and azimuth, ψ, using Eqs. (0.98) and (0.99) is

(0.100) $$v_{x,\psi} = \int_{x_c}^{1}\int_{-\infty}^{\psi}\left[(\Gamma_1\cos\theta)\sqrt{1-\frac{(2xv-x_c-1)^2}{(1-x_c)^2}}\right]\left[\frac{x\sin(\psi-\theta)+\mu(\psi-\theta)\sin\theta}{L^3}\right] d\theta\, dxv$$

It is particularly important to study the integration with respect to wake age, θ, before discussing a complete integration of Eq. (0.100). The reason is that this portion of the integration has a definite possibility of "blowing up." Therefore, reverse Eq. (0.100)'s integration order so that it reads as

(0.101) $$v_{x,\psi} = \int_{-\infty}^{\psi}\left\{\int_{x_c}^{1}\left[(\Gamma_1\cos\theta)\sqrt{1-\frac{(2xv-x_c-1)^2}{(1-x_c)^2}}\right]\left[\frac{x\sin(\psi-\theta)+\mu(\psi-\theta)\sin\theta}{L^3}\right] dxv\right\} d\theta$$

In the first place, the integration *is not* a problem when $\theta = \psi$ because the numerator of the integrand is zero (i.e., $\psi - \theta = 0$). Furthermore, from Eq. (0.95), the distance, L, between the vortex segment and the point on the blade where induced velocity is sought reduces to

$$L^3 = R\left\{\left[xv^2 + x^2 - 2x(xv)\cos(0)\right]\right\}^{\frac{3}{2}} = R\left\{(xv-x)^2\right\}^{\frac{3}{2}}$$

which is only zero when x = xv. The physical meaning of this situation when $\theta = \psi$ is that the only vortex that exists is the blade's bound circulation and this straight-line vortex can not induce a velocity on itself.

Now look at the solution when a shed vortex is in the region $\psi - \theta > 0$ or, if you prefer, in the near wake. Suppose, for example, that the blade is at the 135-degree azimuth and θ is in the range 135 degrees backwards to 132 degrees in 1/30 of a degree increments. This represents three degrees of near wake. Assume the induced velocity is sought at the blade station, x = 0.5, and place the blade at azimuth $\psi = 135$ degrees. The accumulation of the shed wake's influence is

$$\text{area under } \frac{dv_{x,\psi}}{d\theta} \text{ versus } \theta$$

The curve of $\dfrac{dv_{x,\psi}}{d\theta}$ versus wake age is illustrated with Fig. 29. This figure suggests an impending singularity as computations are made very close to the blade. In fact, the velocity induced at the blade station x = 0.5 becomes so large that a semi-log scale for the ordinate on Fig. 29 is helpful in capturing how rapidly the shed wake's influence drops off as the blade moves away from the deposited shed wake.

The common solution to the situation illustrated by Fig. 29 is to add a vortex core diameter, VCD, non-dimensionalized by rotor radius, R, to the L dimension of the shed-wake problem [refer back to the discussion surrounding Eq. (0.62)]. This solution is effective, as Fig. 30 shows. Of course, it is the integrated value

$$v_{x=0.5} = \int_{\frac{\pi}{180}132}^{\psi=\frac{\pi}{180}135} \frac{dv_{x,\psi}}{d\theta} d\theta$$

that is more important, and this integrated result is shown versus vortex core diameter ratioed to radius in Fig. 31 for x = 0.5 and $\psi = 135$ degrees. And even more important is the integrated value of induced velocity considering the wake extending all the way back to, say, $\theta = -20\pi$. The induced velocity at x = 0.5 (and with $\psi = 135$ degrees) including this far wake is also shown on Fig. 31.

To examine the influence of the shed wake further, select, somewhat arbitrarily, the ratio of vortex core diameter to rotor radius equal to 0.015. Now the distance, L, between the vortex segment and rotor-blade station where induced velocity is sought, x, is rewritten as

$$(0.102) \quad L^3 = R \left\{ \begin{array}{l} \left[xv^2 + x^2 - 2x(xv)\cos(\psi-\theta) \right] \\ +2\mu(xv\cos\theta - x\cos\psi)(\psi-\theta) \\ +(\psi-\theta)^2(\mu^2 + \lambda_{tpp}^2) + \left(\dfrac{VCD}{R}\right)^2 \end{array} \right\}^{\frac{3}{2}}$$

38

Mathcad's built-in numerical integrator had absolutely no problem calculating the induced velocity at all radius stations and any azimuth.

$$(0.103) \quad v_{x,\psi} = \int\limits_{x_c}^{1} \int\limits_{-\infty}^{\psi} \left[\left(\Gamma_1 \cos\theta \right) \sqrt{1 - \frac{\left(2xv - x_c - 1 \right)^2}{\left(1 - x_c \right)^2}} \right] \left[\frac{x\sin\left(\psi - \theta \right) + \mu\left(\psi - \theta \right)\sin\theta}{L^3} \right] d\theta \, dxv$$

The calculation could be performed even at x = xv because the distance, L, can never be smaller than VCD/R. Furthermore, because the shed wake's circulation goes smoothly to zero at both the blade root and tip, there is no need to perform a fixed-wing coordinate transformation as was helpful for the trailed wake integration of both fixed and rotary wings.

The next objective is to calculate the induced velocity for the sample problem's geometry and operating condition. To begin the numerical integration, additional input is required, however. The additional input that satisfies rotor lift = 2,712 pounds at an advance ratio of 0.5 is that Γ_o = 334 and Γ_1 = –253.9. For convenience, the complete input for the shed-wake numerical integration is:

$$R = 22 \text{ feet}$$
$$x_c = 1/6 \text{ non-dimensional}$$
$$\rho = 0.002378 \text{ slugs per cubic feet}$$
$$VCD/R = 0.015 \text{ non-dimensional}$$
$$V_t = 603.605 \text{ feet per second}$$
$$\mu = 0.5 \text{ non-dimensional}$$
$$\lambda tpp = -0.03 \text{ non-dimensional}$$
$$\Gamma_o = 334 \text{ square feet per second}$$
$$\Gamma_1 = -253.9 \text{ square feet per second}$$

With this information as input, put Mathcad and its built-in integrator to work calculating Eq. (0.103) as follows:

INPUT

$\mu = 0.5 \quad \Gamma_o = 334 \quad \Gamma_1 = -253.9 \quad R = 22 \quad x_c = 1/6 \quad \lambda_{tpp} = -0.03 \quad VCD/R = 0.015$

Dimension integration.

      Select azimuth station, ψ = variable for this problem

      Extent of wake age, $WA = -20\pi$

      Maximum number of radial stations, $M = 90$

      Range of radial stations where induced velocity is calculated, $s = 0,1.......M-1$

Then proceed with these calculations

$$a = \frac{1-x_c}{2} \qquad\qquad b = \frac{1+x_c}{2}$$

$$\alpha_s = \frac{\pi}{M}\left(s+\frac{1}{2}\right) \Rightarrow \text{To correspond to radius stations used in trailed-wake problem}$$

$$x_s = \frac{r}{R} = \left(\frac{1+x_c}{2}\right) - \left(\frac{1-x_c}{2}\right)\cos\alpha_s = a - b\cos\alpha_s$$

$$v_{s,\psi} = \int_{x_c}^{1}\int_{-\infty}^{\psi}\left[\left(\Gamma_1\cos\theta\right)\sqrt{1-\frac{(2xv-x_c-1)^2}{(1-x_c)^2}}\right]\frac{x\sin(\psi-\theta)+\mu(\psi-\theta)\sin\theta}{R\left\{\begin{array}{l}\left[xv^2+x^2-2x(xv)\cos(\psi-\theta)\right]\\+2\mu(xv\cos\theta-x\cos\psi)(\psi-\theta)\\+(\psi-\theta)^2\left(\mu^2+\lambda_{tpp}^2\right)+\left(\dfrac{VCD}{R}\right)^2\end{array}\right\}^{\frac{3}{2}}}\,d\theta\,dxv$$

$$x_s = a - b\cos\alpha_s$$

      The calculation of induced velocity at the lifting line—as created by the shed vortices from the lifting line—follows from the above scheme. Additionally, lift and horsepower distributions are calculated from

(0.104)

$$\Delta L_{s,\psi} = \left[\rho V_t\left(x_s+\mu\sin\psi\right)R\right]\left\{\left(\Gamma_o+\Gamma_1\sin\psi\right)\sqrt{1-\frac{(2x_s-x_c-1)^2}{(1-x_c)^2}}\right\}\Delta_s \Rightarrow \text{Running Lift}$$

$$L_\psi = \sum_{s=0}^{M-1}\Delta L_{s,\psi} \Rightarrow \text{Single-blade lift at input azimuth}$$

$$\Delta HP_{s,\psi} = \frac{1}{550}v_{s,\psi}\Delta L_{s,\psi} \Rightarrow \text{Running Horsepower}$$

$$HP_\psi = \sum_{s=0}^{M-1}\Delta HP_{s,\psi} \Rightarrow \text{Single-blade Horsepower at input azimuth}$$

$$\text{where } \Delta_s = \left(\frac{1+x_c}{2}\right)\left[\cos\left(\frac{\pi}{M}s\right)-\cos\left(\frac{\pi}{M}(s+1)\right)\right]$$

40

The shed wake significantly contributes to the total induced velocity that the rotor blade sees, primarily over the mid-span portion of the blade. For example, the azimuthal variation in induced velocity at the three radius stations under examination (i.e., x = 0.25, 0.50, and 0.75) is provided by Figs. 32, 33, and 34. It is at the mid-span that the shed wake's additional induced velocity is the greatest.

The blade's azimuthally varying lift for the balanced rotor is illustrated with Fig. 35. Note, in contrast to the unbalanced rotor shown on Fig. 24, the balanced rotor carries lift in the fore and aft quadrants of the revolution. This gives, in effect, a short wing span or low aspect ratio characteristic to the balanced rotor. As Fig. 36 shows, this concentration of balanced rotor lift in the fore and aft direction is accompanied by excessive induced horsepower when compared to the unbalanced rotor of Fig. 24. The average or steady induced horsepower for the balanced rotor is HP_i = 76.4 hp versus 50.1 hp for the unbalanced rotor and versus 6.13 hp for the ideal fixed wing.

The requirement for a rotor to have zero rolling moment is clearly adverse to the induced power required to produce lift. The ratio of balanced rotor-induced horsepower to ideal fixed wing-induced horsepower is 76.4/6.13 = 12.4. But keep in mind that while an elliptical bound circulation is ideal for a fixed wing, it is not *obviously* true for a rotary wing.

V. Closing Remarks

This elementary introduction to induced velocity has been presented assuming an elliptical bound circulation distributed along a lifting line to represent both the wing and the rotor. The assumption has been that

$$\Gamma \propto \sum_1^\infty A_n \sin n\beta$$

and that $A_1 = 1$ while A_2 through $A_\infty = 0$. An extension of the fundamental equations provided by this note could easily be made using a full set of the Fourier series. This extension—if made—would completely generalize the lift distribution for the rotor just as is done in the case of fixed-wing theory.

The lifting rotor's spiraling vortex wake structure leads to very high induced power when compared to the ideal wing. For an advance ratio of 0.50, interference created by the spiraling rotor wake leads—just for a single blade—to induced power on the order of 10 times that of the wing when the comparison is made at wing span = rotor diameter and equal lift. While an elliptical bound circulation is known to be ideal for the fixed wing, it is quite probably not ideal for the rotary wing in high-speed forward flight.

A single-bladed rotor and prescribed wake geometry have been selected for this rotary-wing introduction. This has been useful for an elementary discussion. However, the practical problem includes any number of blades and vortex wake structure that is free to deform based on fundamental principles. Furthermore, representing the rotor blade by a lifting line is quite unsatisfactory when the rotor lift distribution varies with time. Fortunately, advanced analyses coupled with powerful digital computers have given today's rotorcraft engineers insight and practical answers to the effect of a rotor system's wake upon the lifting surfaces that created the wake.

References

1. Potsdam, M.; Yeo, Hyeonsoo; and Johnson, Wayne: Rotor Airloads Prediction Using Loose Aerodynamic/Structural Coupling. Presented at the American Helicopter Society 60th Annual Forum, Baltimore, MD, June 7–10, 2004.

2. Datta, A.; Sitaraman, J.; Chopra, I.; and Baeder, J.: Analysis Refinements for Prediction of Rotor Vibratory Loads in High-Speed Forward Flight. Presented at the American Helicopter Society 60th Annual Forum, Baltimore, MD, June 7–10, 2004.

3. Harris, F. D.; Tarzanin, F. J.; and Fisher, R. K.: Rotor High Speed Performance, Theory Versus Test. Presented at the Air Force Flight Dynamics Laboratory V/STOL Technology and Planning Conference, September 1969 (also AHS Journal, Vol. 15, No. 3, July 1970).

4. Miller, R. H.: Rotor Harmonic Air Loading. Institute of the Aerospace Sciences, IAS Paper No. 62-82, January 1962.

Figure 1

Figure 2

$$X \quad i$$

$$xw \quad xv$$

$$+\frac{b}{2}$$

$$\delta$$

$$L$$

$$dS = \frac{\partial S}{\partial \theta} d\theta$$

$$\gamma_v = -\frac{d\Gamma}{dxv} dxv$$

$$-\frac{b}{2}$$

$$V$$

$$D$$

$$-\theta$$

$$Y \quad j$$

Positive $Z \quad k$
Up

Pylon

Figure 3

$$\gamma_v = \frac{d\Gamma}{dxv}\,dxv$$

$$dS = \frac{\partial S}{\partial \theta}\,d\theta$$

$-\theta$

Y
j

Z
k

Positive
Down

X
i

v

xw

xv

47

Figure 4

48

Figure 5

49

Figure 6

Figure 7

51

Figure 8

Figure 9

Wing span point
at which induced
velocity is sought

Wing Span Station, β, deg

$$\frac{dv}{d\beta}$$

53

Figure 10

Figure 11

$$dS = \frac{\partial S}{\partial \theta} \, d\theta$$

$$\gamma_V = -\frac{d\Gamma}{dxv} \, dxv$$

$+\theta$

L

Ψ

rc

$$Z_V = \frac{dzv}{d\theta} \, d\theta$$

R

rv

r

Y j

X i

Z k

Figure 12

Parameter	Value
Rotor radius, R, feet	30.0
Root cutout, r_c, feet	3.0
Trail vortex from radius, rv, feet	27.0
Calculate induced velocity at radius, r, feet	16.5
Trailed vortex strength, γ_v, ft^2 per second	1,265.0
Vortex descent measure, dzv/dθ, feet per radian	2.0
Wake age, θ_{end}, radians	-157.0
Number of 360-degree spirals	25
Distance from rotor down to last spiral, zv, feet	314

Number of 360-Degree Spirals

Figure 13

Figure 14

58

Rotor Span Station, r, ft

Figure 15

59

Figure 16

Figure 17

Y

Tip Vortex

75% Radius

50% Radius

Root Cutout

B
l
a
d
e

Hub

X

61

Figure 18

62

Figure 19

63

Figure 20

$$dS = \frac{\partial \theta}{\partial \theta} \, dp$$

$$\gamma_{V} = -\frac{d\Gamma}{dxv} \, dxv$$

θ

L

Ψ

Y

X

x

xv

Figure 21

65

Figure 22

Figure 23

Figure 24

Figure 25

Figure 26

70

Figure 27

71

$$\gamma_{V=} - \frac{\partial \Gamma}{\partial \theta} d\theta$$

$$dS = \frac{\partial S}{\partial x_V} dx_V$$

Shed Vortex

θ

Trailed Vortex

L

Ψ

x

Y

X

Figure 28

Wake Age, θ, deg
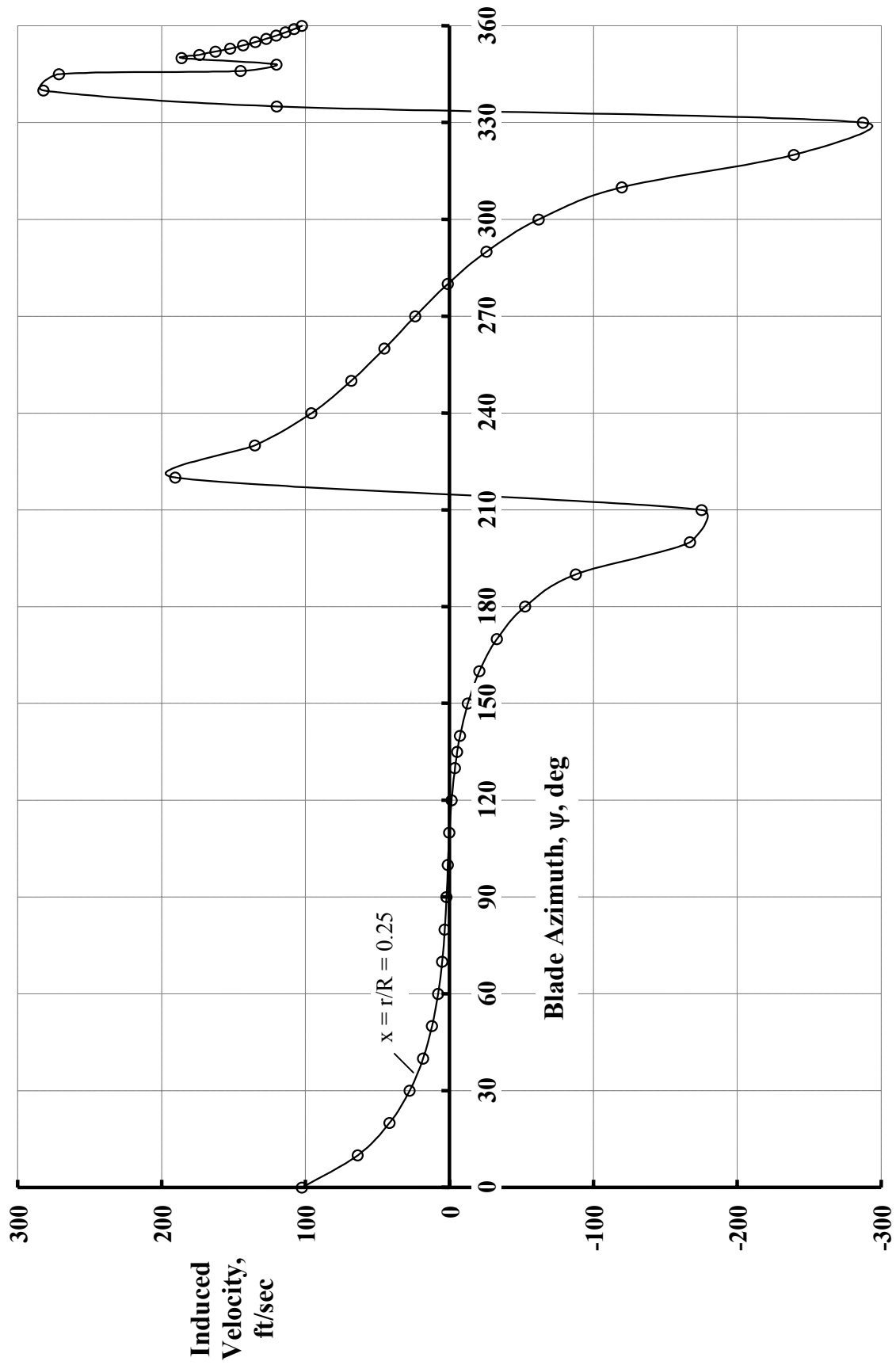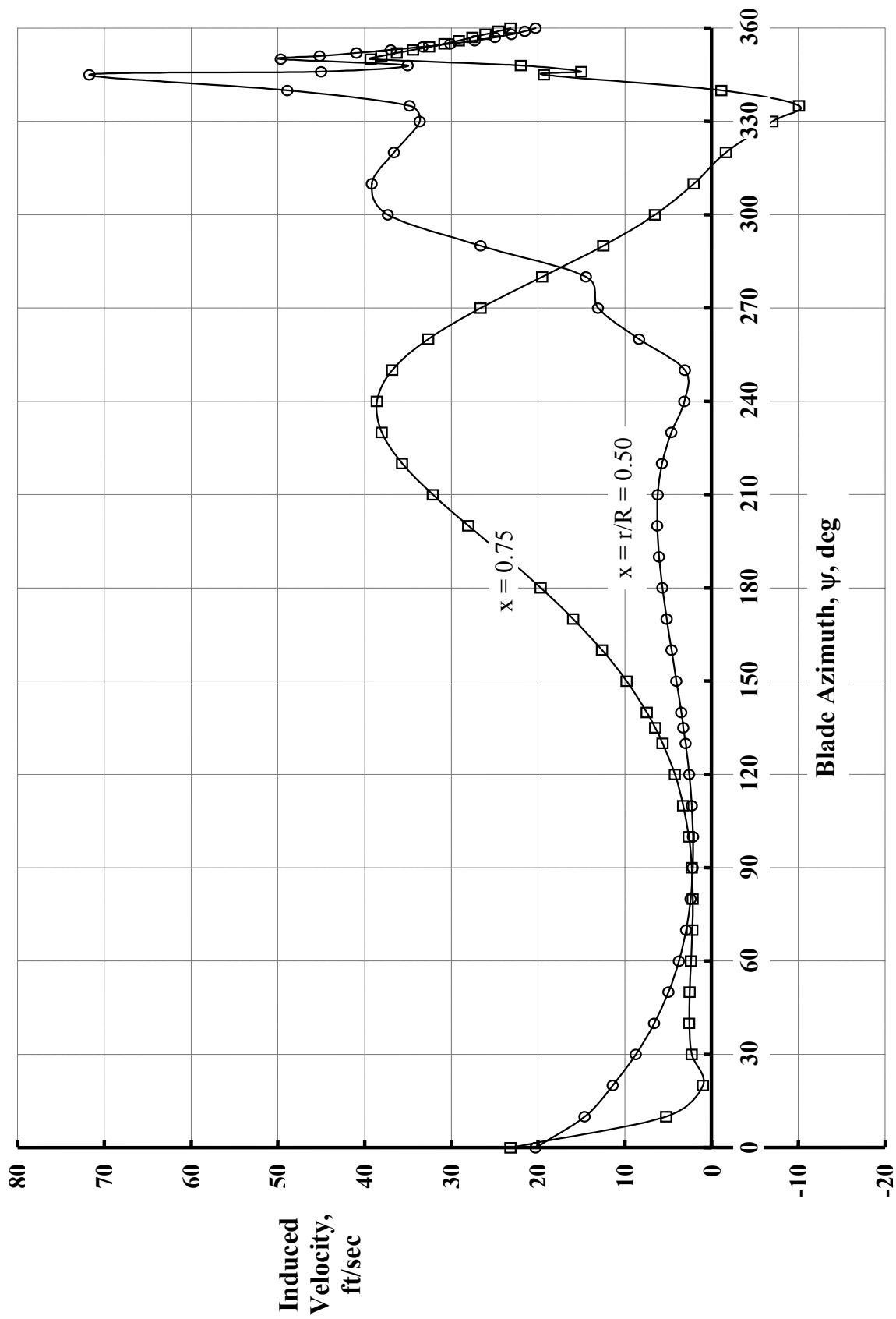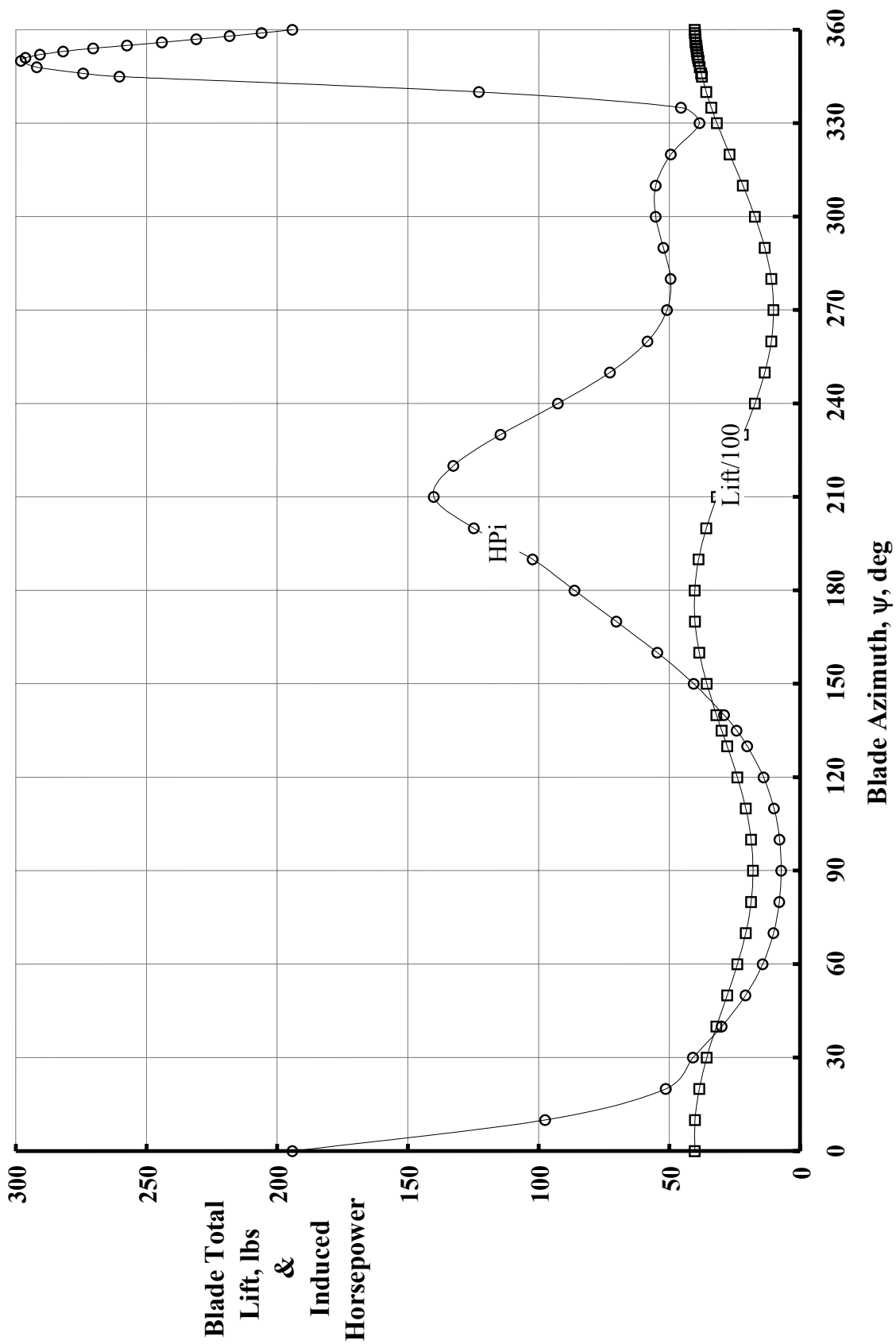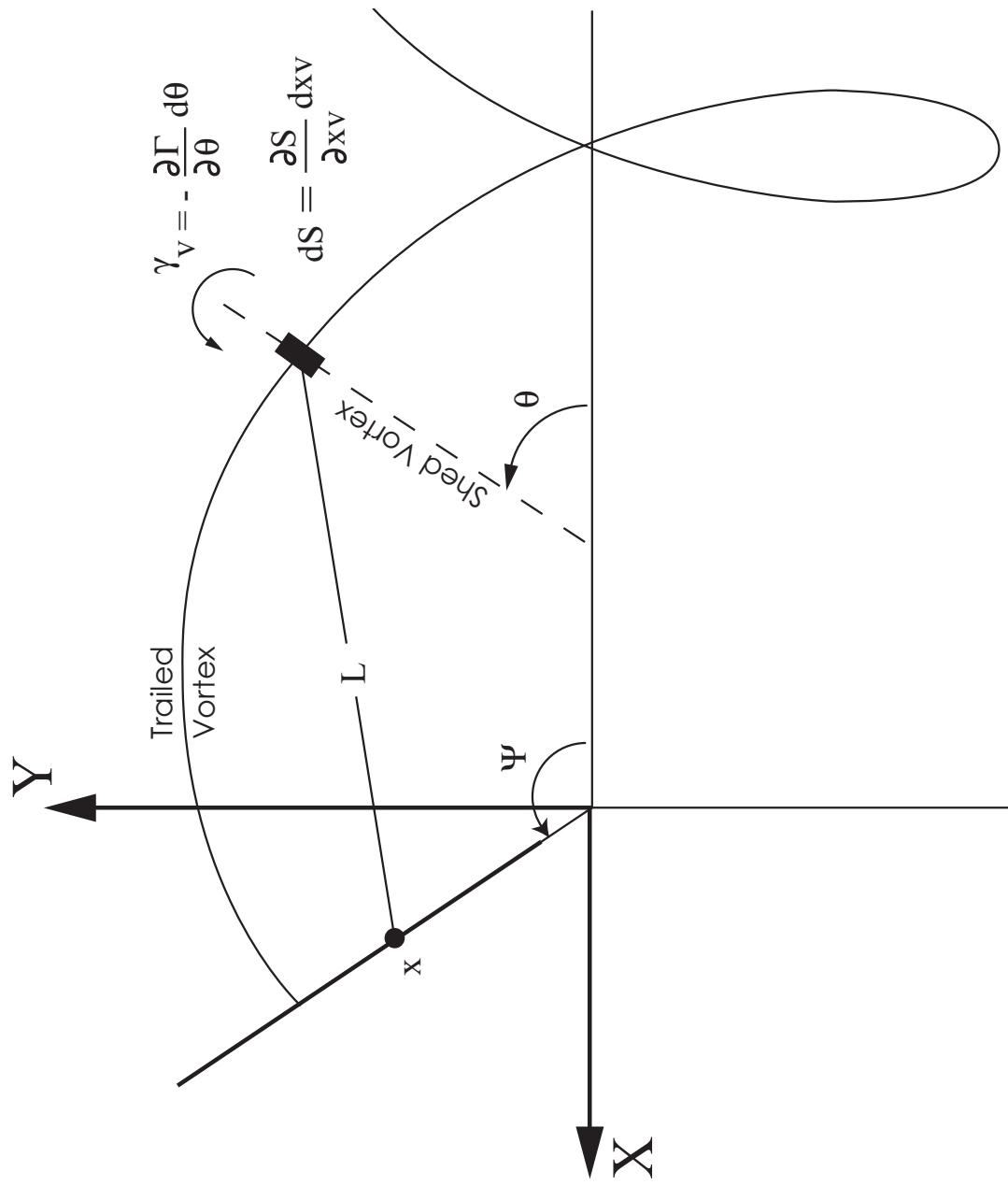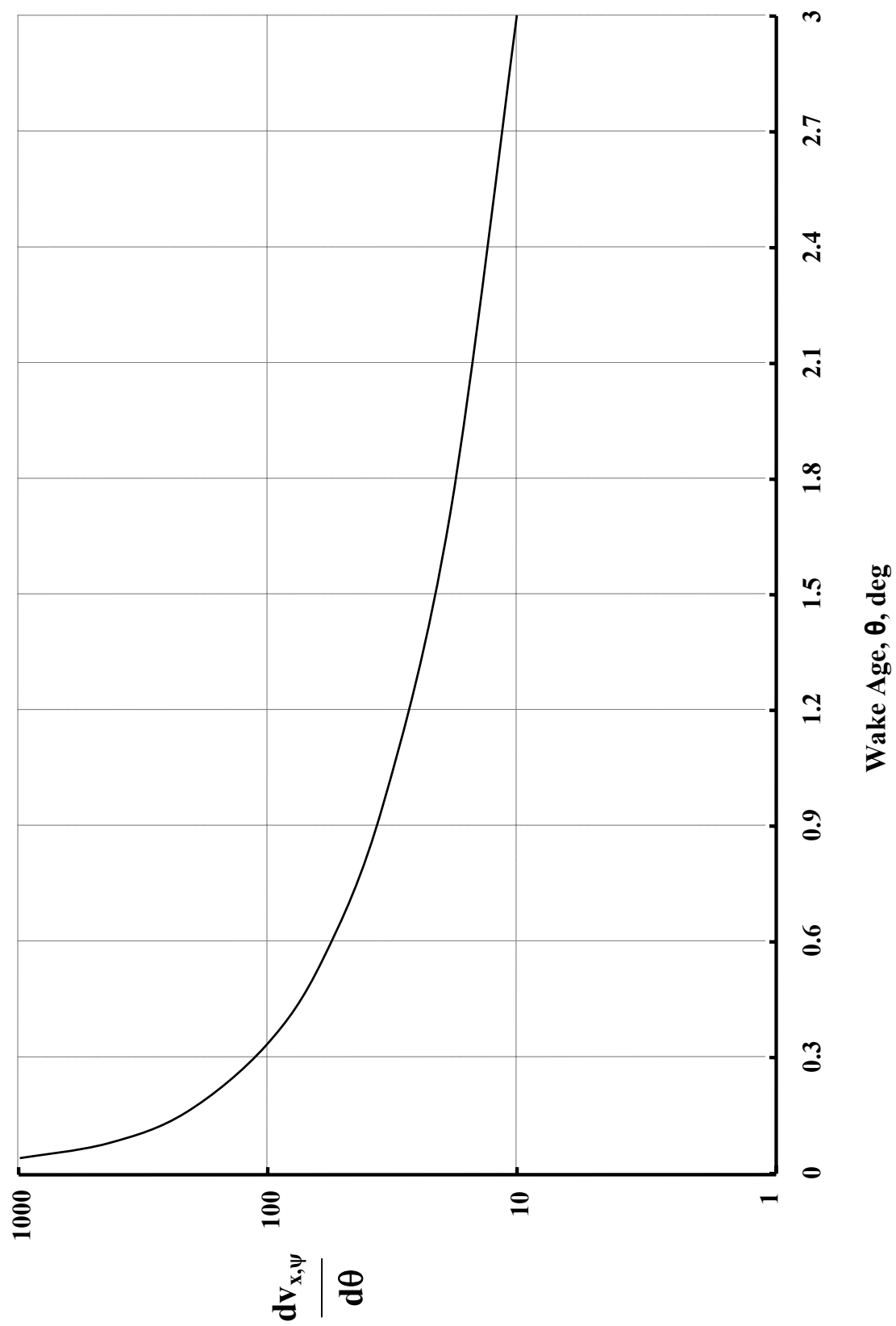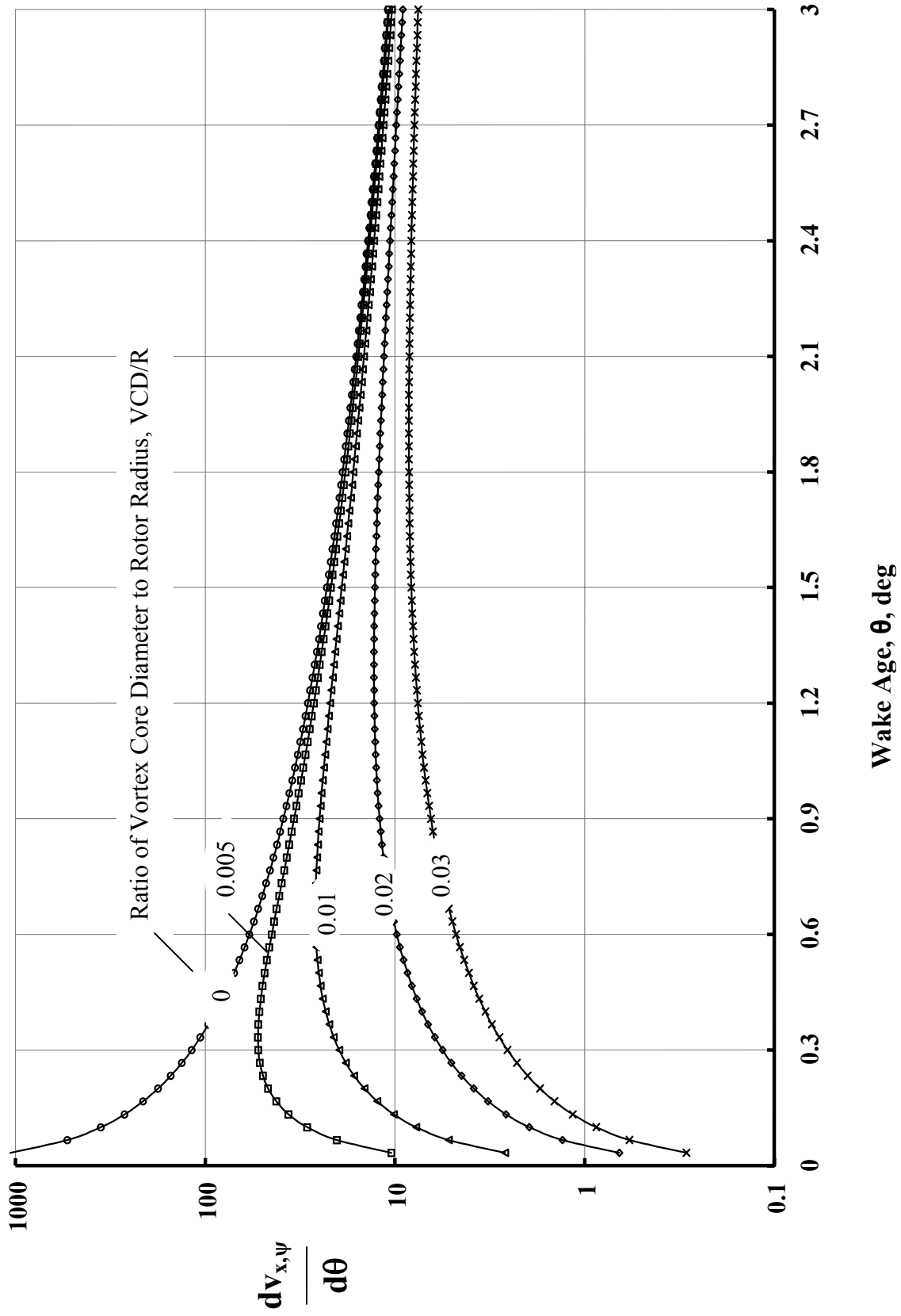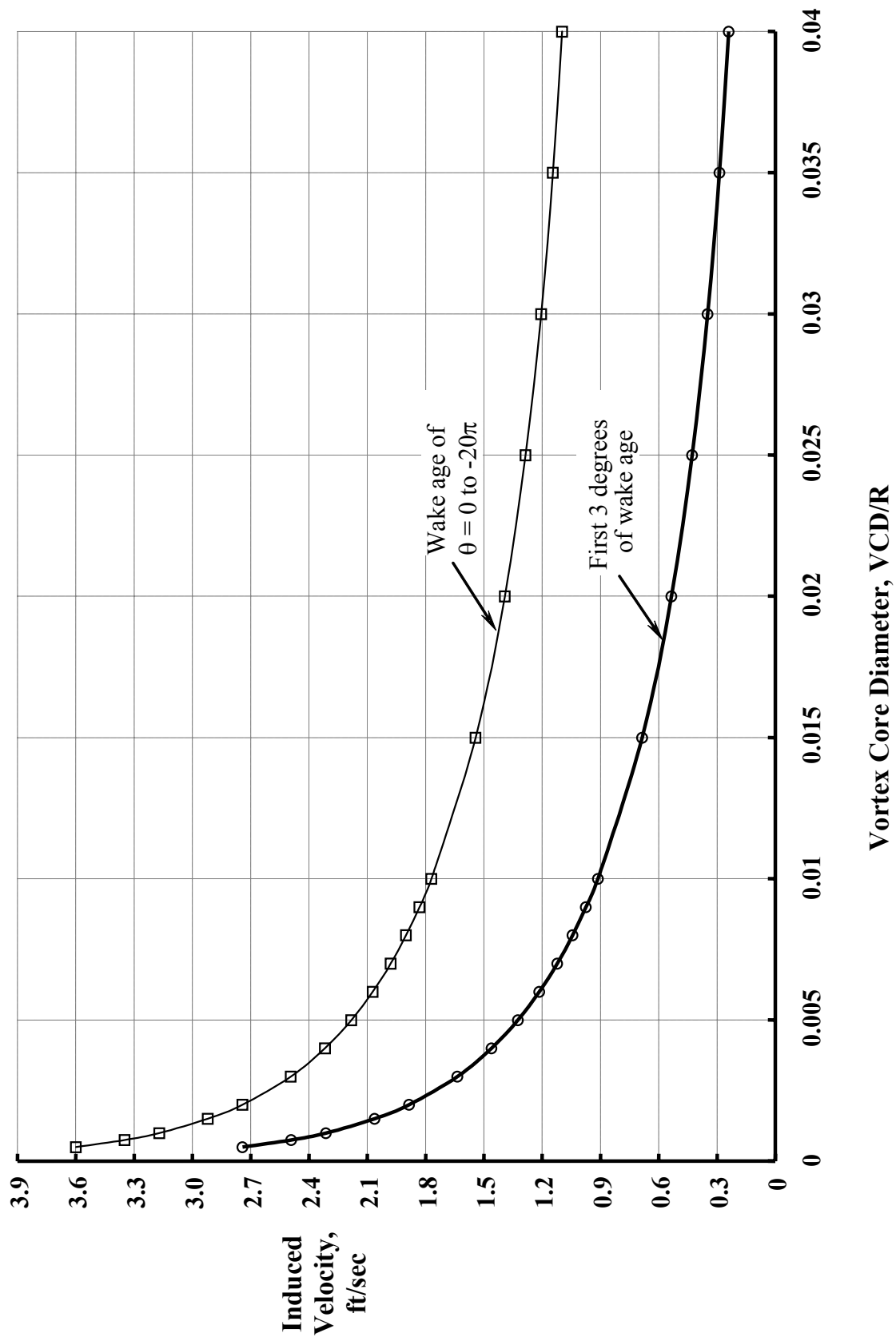
Figure 29

Figure 30

Figure 31

Figure 32

Figure 33

77

Figure 34

78

Rotor Blade Lift, lb

Blade Azimuth, ψ , deg

Figure 35

79

Figure 36

80

1. REPORT DATE *(DD-MM-YYYY)* 15-02-2006	2. REPORT TYPE Contractor Report	3. DATES COVERED *(From - To)* May 2005–Dec 2005

4. TITLE AND SUBTITLE		5a. CONTRACT NUMBER
A Note about Self-Induced Velocity Generated by a Lifting-Line Wing or Rotor Blade		5b. GRANT NUMBER NAG-2-1597
		5c. PROGRAM ELEMENT NUMBER
6. AUTHOR(S) Harris, Franklin D.		5d. PROJECT NUMBER
		5e. TASK NUMBER
		5f. WORK UNIT NUMBER

7. PERFORMING ORGANIZATION NAME(S) AND ADDRESS(ES) University of Maryland Department of Aerospace Engineering College Park, MD 20742-5141 and Ames Research Center, Moffett Field, CA 94035-1000	8. PERFORMING ORGANIZATION REPORT NUMBER A-050006

9. SPONSORING/MONITORING AGENCY NAME(S) AND ADDRESS(ES) National Aeronautics and Space Administration Washington, D.C. 20546-0001	10. SPONSORING/MONITOR'S ACRONYM(S) NASA ARC
	11. SPONSORING/MONITORING REPORT NUMBER NASA/CR-2006-213478

12. DISTRIBUTION/AVAILABILITY STATEMENT
Unclassified—Unlimited   Distribution: Nonstandard
Subject Category: 02
Availability: CASI (301) 621-0390

13. SUPPLEMENTARY NOTES
Point of Contact: Dr. William Warmbrodt, Project Manager, Ames Research Center (Org Code AUA) Moffett Field, CA 94035   650-604-5642

14. ABSTRACT

This report presents an elementary analysis of the induced velocity created by a field of vortices that reside in the wake of a rotor blade. Progress achieved by other researchers in the last 70 years is briefly reviewed. The present work is presented in four stages of complexity that carry a lifting-line representation of a fixed wing into a single-blade rotor. The analysis leads to the conclusion that the lifting rotor's spiraling vortex wake structure has very high induced power when compared to the ideal wing. For an advanced ratio of one-half, induced power is on the order of 10 times that of the wing when the comparison is made at wingspan equal to rotor diameter and wing and rotor having equal lift.

15. SUBJECT TERMS
Rotorcraft aeromechanics, Aerodynamics of rotorcraft, Wing lift, Induced velocity, Rotor wake, Rotor blade, Aerodynamic drag

16. SECURITY CLASSIFICATION OF:			17. LIMITATION OF ABSTRACT	18. NUMBER OF PAGES	19a. NAME OF RESPONSIBLE PERSON William G. Warmbrodt
a. REPORT	b. ABSTRACT	c. THIS PAGE	Unclassified	89	
Unclassified	Unclassified	Unclassified			19b. TELEPHONE *(Include area code)* (650) 604-5642